

1 **Short Title:** Shared genetic control of root traits across taxa

2
3 **Corresponding Author:** Patrick S. Schnable; 2031 Roy J. Carver Co-Laboratory, Iowa State
4 University, Ames, Iowa 50011-3650; Phone: 515-294-0975; Email: schnable@iastate.edu

5
6 **Shared genetic control of root system architecture between *Zea mays* and *Sorghum bicolor***

7
8 **Author Affiliation:**

9
10 Zihao Zheng^{1,2}, Stefan Hey^{1,3}, Talukder Jubery⁴, Huyu Liu^{1,2,5}, Yu Yang^{1,5,6}, Lisa Coffey¹,
11 Chenyong Miao⁷, Brandi Sigmon⁸, James C. Schnable⁷, Frank Hochholdinger³, Baskar
12 Ganapathysubramanian⁴ and Patrick S. Schnable^{1,2,5}

13
14 ¹ Department of Agronomy, Iowa State University, Ames, IA 50011-1051, USA;

15 ² Interdepartmental Genetics and Genomics Graduate Program, Iowa State University, Ames, IA
16 50011-3650, USA;

17 ³ INRES, Institute of Crop Science and Resource Conservation, Crop Functional Genomics,
18 University of Bonn, Bonn 53113, Germany;

19 ⁴ Department of Mechanical Engineering, Iowa State University, Ames, IA 50011-2030, USA;

20 ⁵ Department of Plant Genetics & Breeding, China Agricultural University, Beijing 100193,
21 China;

22 ⁶ Current Address: Annoroad Gene Technology, Beijing 100176, China;

23 ⁷ Department of Agronomy and Horticulture, University of Nebraska-Lincoln, Lincoln, NE
24 68583-0915, USA;

25 ⁸ Department of Plant Pathology, University of Nebraska-Lincoln, Lincoln, NE 68583-0915,
26 USA;

27
28 **One-sentence summary:** Comparisons between root system architecture-associated genes
29 identified from maize and sorghum via GWAS enabled by high-throughput phenotyping reveal
30 conserved functional roles of syntenic orthologs.

31
32 **Author Contributions:** Z.Z., S.H., D.N., J.C.S., B.G. and P.S.S. conceived and designed the
33 experiments; T.J. developed image analysis software; L.C. proposed the use of the Airspade;
34 Z.Z., S.H., T.J., H.L., Y.Y., L.C. and B.S. provided experimental materials, collected data and/or
35 performed experiments; Z.Z., S.H., T.J., C.M., F.H., J.C.S., and P.S.S. analyzed and interpreted

36 data; Z.Z., S.H., J.C.S., and P.S.S wrote and edited the manuscript with input from T.J., B.S.,
37 F.H., and B.G.

38
39 **Funding information:** The information, data, or work presented herein was funded in part by
40 the Advanced Research Projects Agency-Energy (ARPA-E), U.S. Department of Energy, under
41 Award Number DE-AR0000826.

42
43

44
45 **Abstract**

46
47 Determining the genetic control of root system architecture (RSA) in plants via large-scale
48 genome-wide association study (GWAS) requires high-throughput pipelines for root
49 phenotyping. We developed CREAMD (Core Root Excavation using Compressed-air), a high-
50 throughput pipeline for the cleaning of field-grown roots, and COFE (Core Root Feature
51 Extraction), a semi-automated pipeline for the extraction of RSA traits from images. CREAMD-
52 COFE was applied to diversity panels of maize (*Zea mays*) and sorghum (*Sorghum bicolor*),
53 which consisted of 369 and 294 genotypes, respectively. Six RSA-traits were extracted from
54 images collected from >3,300 maize roots and >1,470 sorghum roots. SNP-based GWAS
55 identified 87 TAS (trait-associated SNPs) in maize, representing 77 genes and 115 TAS in
56 sorghum. An additional 62 RSA-associated maize genes were identified via eRD-GWAS.
57 Among the 139 maize RSA-associated genes (or their homologs), 22 (16%) are known to affect
58 RSA in maize or other species. In addition, 26 RSA-associated genes are co-regulated with genes
59 previously shown to affect RSA and 51 (37% of RSA-associated genes) are themselves *trans*-
60 eQTL for another RSA-associated gene. Finally, the finding that RSA-associated genes from
61 maize and sorghum included seven pairs of syntenic genes demonstrates the conservation of
62 regulation of morphology across taxa.

63
64

65 **Key Words:** root system architecture; high-throughput phenotyping; syntenic orthologs

66
67
68
69
70

71 **Introduction**

72

73 The spatial arrangements of root systems, i.e., root system architecture (RSA) (Lynch, 1995),
74 plays a critical role in plant productivity and tolerance to environmental stresses. In maize (*Zea*
75 *mays*), the majority of the root mass is found in the top 0.3 m of soil (Amos and Walters, 2006).
76 This mass of roots has been referred to as the “root crown” (Trachsel *et al.*, 2011), the “core root”
77 (Grift *et al.*, 2011), or the “core root system” (Hauck *et al.*, 2015). The term core root system is
78 used hereafter for two reasons. First, the term root crown originally referred only to the above-
79 ground portion of the root system (Schwarz, 1972; Bray *et al.*, 2006). Only more recently has this
80 term been used to describe roots within the top 0.3 m of soil (Trachsel *et al.*, 2011). Second, this
81 term is easily confused with the term “crown roots”, which refers to post-embryonic shoot-borne
82 roots (Kiesselbach, 1949).

83

84 The genetic regulation of root development has been extensively studied in *Arabidopsis* (Dolan
85 *et al.*, 1993; Birnbaum *et al.*, 2003; Petricka *et al.*, 2012; Petricka *et al.*, 2013) resulting in an in-
86 depth understanding of the relevant genes and pathways. Despite similarities in embryonic root
87 systems and some shared mechanisms of genetic regulation, there are major anatomical
88 differences between the root systems of *Arabidopsis* and cereal crops. The adult *Arabidopsis* root
89 system comprises a tap root, a basal root, hypocotyl roots, internodal shoot-borne roots, and
90 lateral roots (Zobel, 2016). By contrast, the maize root system is composed of the embryonic
91 primary root and variable numbers of seminal roots, as well as postembryonic shoot-borne and
92 lateral roots (Hochholdinger and Tuberosa, 2009). Similar to maize, sorghum (*Sorghum bicolor*)
93 develops shoot-borne roots; however, sorghum lacks seminal roots (Singh *et al.*, 2010). Based on
94 these fundamental morphological differences, it is unlikely that a complete understanding of the
95 genetic regulation of RSA in these species can be elucidated from *Arabidopsis*.

96

97 Whereas functional studies on qualitative mutants of genes with large effect sizes have deepened
98 our understanding of the genetic control and developmental processes of the root systems of
99 cereals, a comprehensive understanding of the genes underlying quantitative variation in RSA
100 has not been achieved (Hochholdinger *et al.*, 2018).

101

102 Genome-wide associated study (GWAS) offers the opportunity to identify genes affecting
103 natural variation of quantitative traits via the association of markers across the genome with
104 phenotypic variation within diversity panels (Xiao et al., 2017). With the ready availability of
105 large numbers of genetic markers, phenotyping has become the bottleneck for GWAS. Several
106 root phenotyping pipelines have been developed for genetic mapping (Topp et al., 2013; Zurek et
107 al., 2015). Most of these studies were conducted on young plants grown in microcosms and
108 mesocosms (Topp, 2016). However, it has been observed in multiple species that RSA varies
109 across development and environments (Rauh et al., 2002; Magalhaes et al., 2004; Trachsel et al.,
110 2013) and that roots grown under controlled conditions do not match those grown under field
111 conditions (Poorter et al., 2016). Hence, if we wish to understand the genetic control of RSA as it
112 relates to crop growth in target environments, it is necessary to phenotype roots grown under
113 agronomically relevant field conditions. However, the throughput of current pipelines for
114 analyzing RSA is insufficient to satisfy the phenotyping needs of large-scale GWAS. Hence,
115 thus far, efforts to characterize RSA have mainly focused on quantitative trait locus (QTL)
116 mapping using bi-parental populations with limited genetic diversity, population size, and
117 mapping resolution (Thomson et al., 2003; Giuliani et al., 2005; Li et al., 2005; Liang et al., 2010;
118 Cai et al., 2012; Atkinson et al., 2015; Richard et al., 2015; Guo et al., 2018). To date, few of the
119 genes underlying RSA QTL in cereal crops have been cloned (Mai et al., 2014; Hochholdinger et
120 al., 2018).

121
122 Maize and sorghum are both important crops, ranked first and fifth, respectively, in global cereal
123 production (<http://faostat.fao.org/>). Maize and sorghum diverged from a common ancestor
124 approximately 12 mya (Swigoňová et al., 2004). Approximately 60% of annotated genes are
125 syntenically conserved between these two species and this syntenically conserved set of genes
126 accounts for >90% of all genes characterized by forward genetics in maize (Schnable and
127 Freeling, 2011; Schnable, 2015). Syntenic orthologs are more likely to retain consistent patterns
128 of gene regulation and expression across related species (Davidson et al., 2012), and may be
129 more likely to retain ancestral functional roles than non-syntenic gene copies (Dewey, 2011).
130 However, to date, the conservation of functional roles for syntenic orthologous gene pairs in
131 related species has not been widely tested.

132

133 We report the development of CREAMD (Core Root Excavation using Compressedair), a high-
134 throughput pipeline suitable for the excavation and cleaning of field-grown roots, and COFE
135 (Core Root Feature Extraction), a semi-automated pipeline to extract features from images of
136 roots. CREAMD-COFE was used to phenotype roots from maize and sorghum diversity panels.
137 Comparative analyses of maize and sorghum GWAS results provided strong evidence for shared
138 genetic control of RSA in these two species and the conservation of functional roles for syntenic
139 orthologous gene pairs.

140

141

142 **Results**

143

144 **CREAMD-COFE enables the efficient excavation, cleaning, and phenotyping of core root**
145 **systems**

146 Manual excavation and cleaning of field-grown roots is labor intensive (Trachsel et al., 2011;
147 Colombi et al., 2015). To simplify the phenotyping of RSA from field-grown plants and thereby
148 enable large-scale genetic studies under agronomic conditions, we developed CREAMD, a
149 pipeline for the rapid excavation and cleaning of roots. CREAMD uses compressed air to remove
150 soil from core root systems (Supplemental Text S1; Figure 1; Methods).

151

152 Following excavation and cleaning, core root systems were photographed (Figure 1; Methods).
153 COFE, a semi-automated pipeline, was used to extract traits from the resulting images
154 (Supplemental Text S1). COFE is an adaptation of the ARIA software (Pace et al., 2014), which
155 had been developed for lab-based phenotyping of immature root systems.

156

157 There are two major potential sources of error between auto-extracted trait values and ground
158 truth: 1) errors introduced via the projection of 3D traits onto a 2D image; and 2) errors in the
159 extraction of trait values from 2D images. To distinguish between these two potential sources of
160 error, we compared COFE-extracted trait values to trait values obtained by manually measuring
161 3D core root systems (ground truth) and to trait values manually extracted (using ImageJ) from
162 2D photos of the same core root systems. These comparisons were performed for approximately
163 5% of all collected maize and sorghum core root systems (Methods). The coefficient of
164 determination (r^2) between COFE's auto-extraction trait values and manual measurements of
165 maximum width and depth from 3D core root systems are 0.54 and 0.46, respectively. By
166 contrast, the r^2 for the same two traits between COFE's auto-extracted trait values and
167 measurements obtained using ImageJ from photos are 0.88 and 0.87, respectively (Supplemental
168 Figure S1; Methods). These results demonstrate that COFE can accurately extract trait values
169 from 2D images of core root systems (Figure 1) and that much of the difference between COFE-
170 extracted trait values and ground truth is due to the challenge of representing 3D core root
171 systems in 2D images.

172

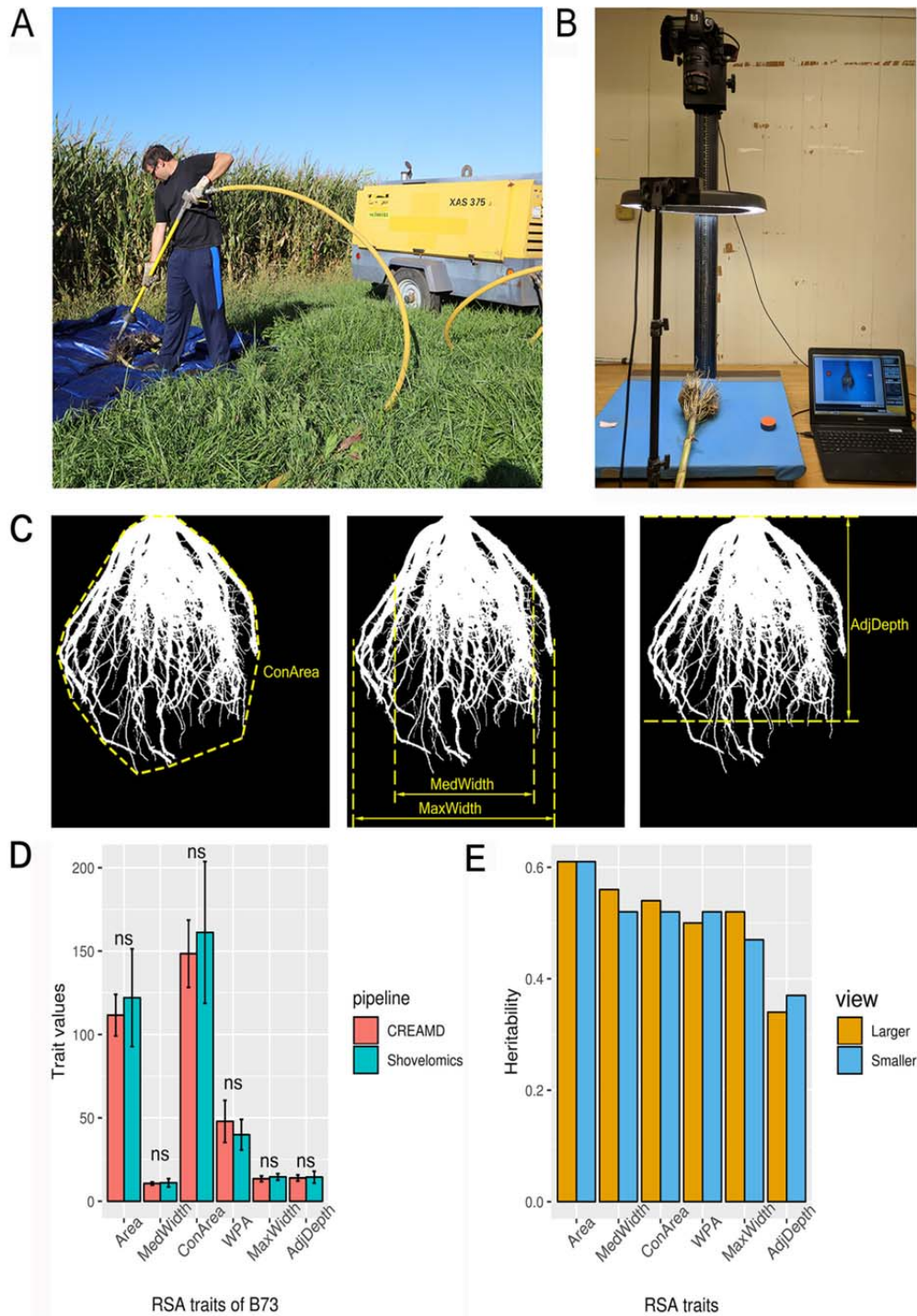


Figure 1: **Extraction of RSA traits from binary images of core root systems using COFE.** A) Illustration of root cleaning and B) phenotyping of CREAMD pipeline; C) Illustration of four out of six traits extracted via COFE; D) Comparison of RSA trait values from the inbred line B73 extracted by COFE from roots collected using CREAMD or water-based root cleaning. Bars indicate mean \pm SD; Student's t-test; n=15; E) Heritabilities of RSA trait values obtained from the SAM Diversity Panel via CREAMD COFE; n=3,196 roots per view.

173 The air-based root cleaning pipeline, CREAMD, increases the speed of root cleaning 6.5-fold as

174 compared to a previously described (Trachsel et al., 2011) water-based root cleaning pipeline
175 (Supplemental Table S1), while yielding comparably intact core root systems; trait values
176 obtained from 15 plants of each of four maize genotypes via CREAMD-COFE (Methods) are
177 similar to those obtained via the water-based root cleaning pipeline (Figure 1; Supplemental
178 Figure S2). In addition to being substantially faster than the water-based root cleaning pipeline
179 without comprising root quality, CREAMD can be conducted at remote field sites that lack
180 access to water.

181

182 **Phenotypic variation of RSA in maize**

183 Three biological replications of 369 inbred lines from the SAM Diversity Panel (Leiboff et al.,
184 2015) were grown (Methods). Core root systems from up to three competitive plants (Methods)
185 from each of the three replications were excavated and cleaned using CREAMD. Each core root
186 system was first photographed using a camera angle selected to obtain a view from a neighboring
187 plant in the row in which the plant under analysis was grown (view 1) and then again after
188 rotating the core root system by 90° (clockwise when viewing from above), resulting in view 2
189 (Methods). Trait values of core root systems of maize from the two views did not exhibit
190 statistically significant differences (Supplemental Table S2), suggesting maize plants do not
191 substantially alter their RSA in response to neighbors, at least at the planting densities employed
192 here (Methods). Even so, when viewed from above core root systems do not exhibit radial
193 symmetry (Supplemental Figure S3; Methods). Consequently, for subsequent analyses, we
194 classified the two images of each core root system as the larger and smaller on a *per trait* basis
195 (Supplemental Figure S4; Supplemental Table S3; Methods).

196

197 COFE was used to extract the following six types of traits from both images of each core root
198 system (Table 1; Figure 1; Supplemental Text S2; Supplemental Figure S4-6). Because we
199 extracted traits from both images of each root, a total of twelve traits were extracted. Maximum
200 and median widths (designated *smMaxWidth*, *lgMaxWidth*, *smMedWidth*, and *lgMedWidth*)
201 served as measures of the horizontal expansion of core root systems. The Adjusted Depth
202 (*smAdjDepth* and *lgAdjDepth*), which is the root depth at which the ratio of root pixels to total
203 pixels exhibits the highest heritability (Supplemental Figure S5) was used a measure of the depth
204 of the core root system. Convex hull (*smConArea* and *lgConArea*), the minimum set of points

205 that define a polygon containing all the pixels of a core root in an image, was used to describe
206 the overall expansion of a core root system. The penultimate trait was total root area (*smArea*
207 and *lgArea*), which is the total number of pixels of roots in a photograph.

208
209 The final extracted trait was root angle. The scientific literature does not offer a consistent
210 definition of root angle, particularly among, but even within, species (Vitha et al., 2000; Li et al.,
211 2005; Hargreaves et al., 2009; Singh et al., 2010; Courtois et al., 2013; Richard et al., 2015),
212 among developmental stages (Omori and Mano, 2007; Fang et al., 2009; Trachsel et al., 2011;
213 Pace et al., 2014; Zurek et al., 2015) and across environments (Topp et al., 2013; Uga et al., 2013;
214 Huang et al., 2018). Due to the low heritabilities (<0.2) of two previously defined measures of
215 root angle (CA) and top angle (IAngRt) (Trachsel *et al.*, 2011; Colombi *et al.*, 2015), we defined
216 a root angle trait based on width profiles (*smWPA* and *lgWPA*). High values of *WPA* are
217 associated with steep roots. *WPA* exhibits higher heritabilities (0.50 for *lgWPA* and 0.52 for
218 *smWPA*) than the two previously described root angle traits (Figure 1; Supplemental Text S2;
219 Supplemental Figure S6).

220
221 The heritabilities of the twelve traits ranged from 0.47 for *smMaxWidth* to 0.61 for *smArea* and
222 *lgArea*, with the exception of *smAdjDepth* and *lgAdjDepth*, which had the lowest heritabilities
223 (0.33 and 0.37) (Figure 1). For five of the six types of root traits (*Area*, *ConArea*, *MedWdith*,
224 *MaxWidth*, *Adjusted Depth*) the two views (large and small) were positively correlated.
225 Correlations between larger and smaller views of the collected RSA traits range from 0.92 for
226 *MaxWidth* to 0.98 for *Area* (Supplemental Table S4). The pair-wise Pearson correlation
227 coefficients ranged from 0.45 (between *smAdjustedDepth* and *smMedWidth*) to 0.97 (between
228 *smArea* and *smConArea*). Both views of *WPA* exhibited negative correlations with all other RSA
229 traits (Supplemental Table S5).

230
231 To determine correlations between RSA and above-ground traits, we compared the 12 RSA traits
232 with four above-ground traits: plant height, plant ear height, flowering time (days to anthesis;
233 DTA), and node number data from Leiboff et al. (2015). Even though the root and above-ground
234 traits were collected in different environments, both views of five of the six types of root traits
235 (*Area*, *ConArea*, *MedWdith*, *MaxWidth*, *Adjusted Depth*) were positively correlated with all four

236 above-ground traits. Pairwise Pearson correlation coefficients ranged from 0.36 (between
237 *smMaxWidth* and node number) to 0.59 (between *lgArea* and *plant ear height*). Similarly, both
238 views of *WPA* exhibited negative correlations with all four above-ground traits (Supplemental
239 Table S5). These correlations between RSA and above-ground traits support the hypothesis that
240 by selecting for the latter breeders may have inadvertently selected for the former.

241

242 **GWAS for RSA traits**

243 FarmCPU accounts for kinship and population structure in GWAS (Liu et al., 2016). An efficient
244 implementation of FarmCPU termed FarmCPUpp (Kusmec and Schnable, 2018) was used to
245 perform GWAS on the SAM Diversity Panel, which was previously genotyped with ~1.2 M
246 SNPs (Leiboff et al., 2015). RSA trait values were adjusted to account for field-based spatial
247 variation (Methods). 107 significant SNPs were associated with six types of RSA traits (each of
248 which has two views, resulting in a total of 12 traits) using an FDR cutoff of < 0.05 (Benjamini
249 and Hochberg, 1995) (Supplemental Table S6). Only 20% (20/107) of these trait-associated
250 SNPs (TASs) were associated with both views of the same trait (i.e., 10 pairs of TASs), a result
251 that is consistent with our finding that roots do not exhibit radial symmetry (Supplemental Figure
252 S3). In addition, ~6% (7/107) of the TASs were associated with two or more traits, a result
253 consistent with the high correlations among traits (Supplemental Table S4). For 77/87 of the
254 TASs (88%) it was possible to identify a candidate gene (“SNP-genes”), which was defined as
255 the gene nearest a TAS within a 20-kb window centered on that TAS (Supplemental Table S6).

256

257 A SNP located within GRMZM2G148937, *Big embryo 1 (Bige1)* (Figure 2), was associated with
258 the trait *smWPA*. *Bige1*, which encodes a MATE transporter, is one of only eight cloned maize
259 genes with a known function in root development (Hochholdinger et al., 2018). A loss-of-
260 function mutant of *Bige1* displays increased number of seminal roots and lateral organs during
261 vegetative development as compared to wild-type controls (Suzuki et al., 2015). Within the SAM
262 Diversity Panel, inbred lines that carry the ALT (i.e., the non-B73) allele of *Bige1* have
263 significantly higher mean values of *smWPA* ($p = 0.01$) than those that carry the REF (i.e., the
264 B73) allele (Figure 2). Based on published trait data (Leiboff et al., 2015), inbred lines
265 homozygous for the ALT allele of *bige1* were shorter and flowered earlier than those
266 homozygous for the REF allele, a result consistent with those of Suzuki et al. (2015). Inbred

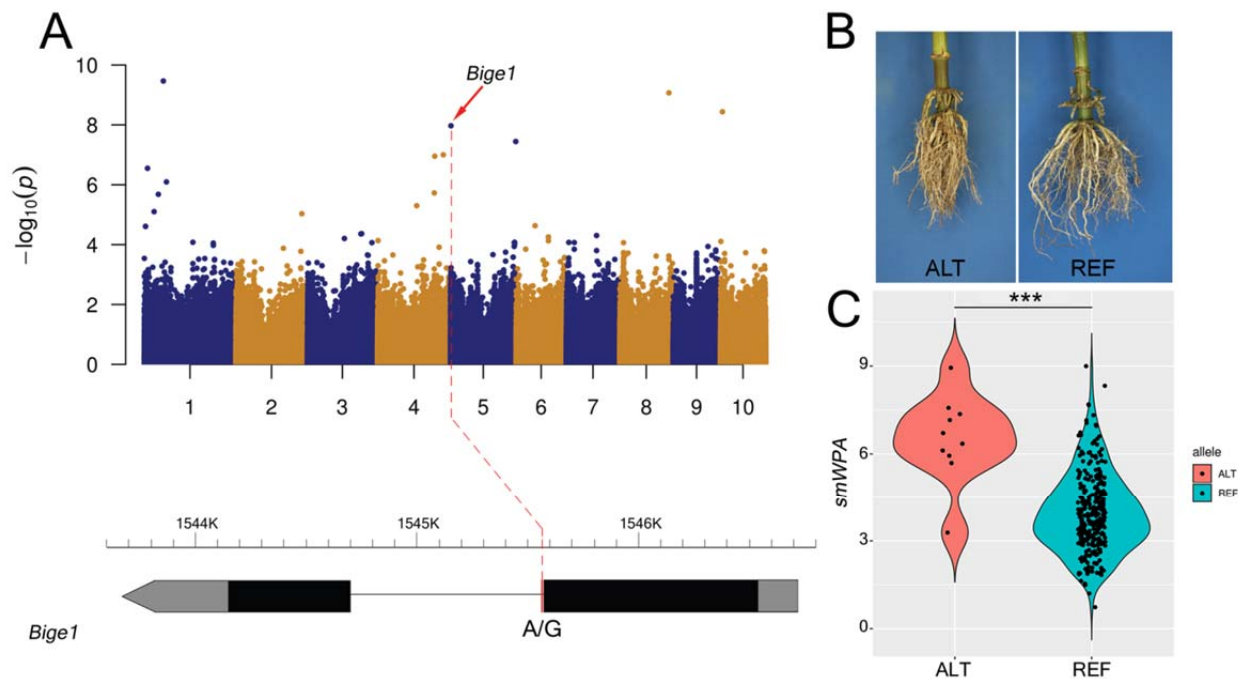


Figure 2: **Association of *Bige1* (GRMZM2G148937) with maize *smWPA*.** A) Manhattan plot of SNP-based GWAS for *smWPA*; Gene model with the position indicated of the RSA-associated SNP within the intron; B) Representative root images of inbred lines homozygous for the ALT (non-B73) and REF (B73) alleles of the RSA-associated SNP within *Bige1*. Illustrated inbred lines are LH52 (ALT allele) and LH57 (REF allele). C) Distribution of trait values of inbred lines homozygous for the ALT and REF alleles. Student's t-test; stars indicate $p < 0.001$.

267 lines homozygous for the ALT allele of *bige1* also exhibit reduced ear height and plant height
 268 (Supplemental Figure S7). In addition, based on published shoot apical meristem (SAM)
 269 phenotypic data (Leiboff et al., 2015), inbred lines that carry the ALT allele of *Bige1* have SAMs
 270 with larger radii. This is consistent with a previous report that SAM radius is correlated with
 271 flowering time, ear height, and plant height (Leiboff et al., 2015).

272
 273 Homologs from other species for 10 of the remaining 76 SNP-genes (13%) are known to
 274 influence RSA (Supplemental Table S7). For example, GRMZM2G143756, a maize homolog of
 275 an Arabidopsis ABCG transporter, was associated with *lgArea*. Members of a clade of five
 276 Arabidopsis ABCG transporters are required for the synthesis of an effective suberin barrier in
 277 roots, and seedlings of the *abcg2 abcg6* and *abcg20* triple mutant of Arabidopsis exhibit fewer
 278 lateral root primordia and fewer lateral roots than wild-type controls (Yadav et al., 2014). In

279 potato (*Solanum tuberosum*), ABCG1-RNAi plants exhibit reduced suberin content in root
280 exodermis cells and tuber periderm cells. The lower suberin content leads to reduced root
281 volume (Landgraf *et al.*, 2014). GRMZM2G013128, a maize homolog of the Arabidopsis
282 *SMXL3* gene, was associated with variation in both the *smMaxWidth* and *lgMedWidth* traits. In
283 Arabidopsis, *SMXL3* is highly expressed in root vasculature; double mutants of *smxl3;smxl4* and
284 *smxl3;smxl5* exhibit reduced primary root lengths as compared to wild-type controls (Wallner *et*
285 *al.*, 2017). GRMZM2G013324, a maize homolog of Arabidopsis *SHV3*, was associated with
286 variation in the trait *lgMaxWidth*. *SHV3* encodes a glycerophosphoryl diester phosphodiesterase
287 (GPDP)-like protein. A mutant of *shv3* exhibits a defective root hair phenotype (Jones *et al.*,
288 2006). GRMZM2G400907, a maize homolog of *GTE4* in Arabidopsis, was associated with
289 variation in *smMedWidth*. *GTE4* is a Bromodomain and Extra Terminal domain (BET) factor,
290 which functions in the maintenance of the mitotic cell cycle. An Arabidopsis mutant of *gte4*
291 exhibits significant shorter primary roots and defective lateral roots (Airoldi *et al.*, 2010).

292

293 **eRD-GWAS of maize RSA**

294 Conventional GWAS uses SNPs as the explanatory variable. By contrast, eRD-GWAS uses gene
295 expression levels as the explanatory variables to associate genes with phenotypic variation (Lin
296 *et al.*, 2017). Because eRD-GWAS has been shown to identify gene/trait associations that are
297 complementary to those identified via SNP-based GWAS (Lin *et al.*, 2017), we also conducted
298 eRD-GWAS.

299

300 RNA-Seq data from 2 cm tips of germinating seedling roots are available for a subset (N=246) of
301 the SAM Diversity Panel (Kremling *et al.*, 2018). eRD-GWAS was conducted on this subset of
302 the SAM Diversity Panel, resulting in the identification of 62 gene-trait associations
303 (Supplemental Table S8). 34% (21/62) of “eRD-genes” are associated with more than two RSA
304 traits, whereas 42% (26/62) are associated with the two views of the same RSA traits. For
305 example, GRMZM2G021410, which encodes a putative alpha/beta-hydrolase superfamily
306 protein, is associated with all six root traits. 12 of the 62 unique eRD-genes (19%) have
307 homologs in Arabidopsis or *Medicago truncatula* with known functions in root development
308 (Supplemental Table S9). For example, Arabidopsis homologs of four eRD-genes associated
309 with variation in the smaller view of root area (*smArea*) of maize (Figure 3) have been associated

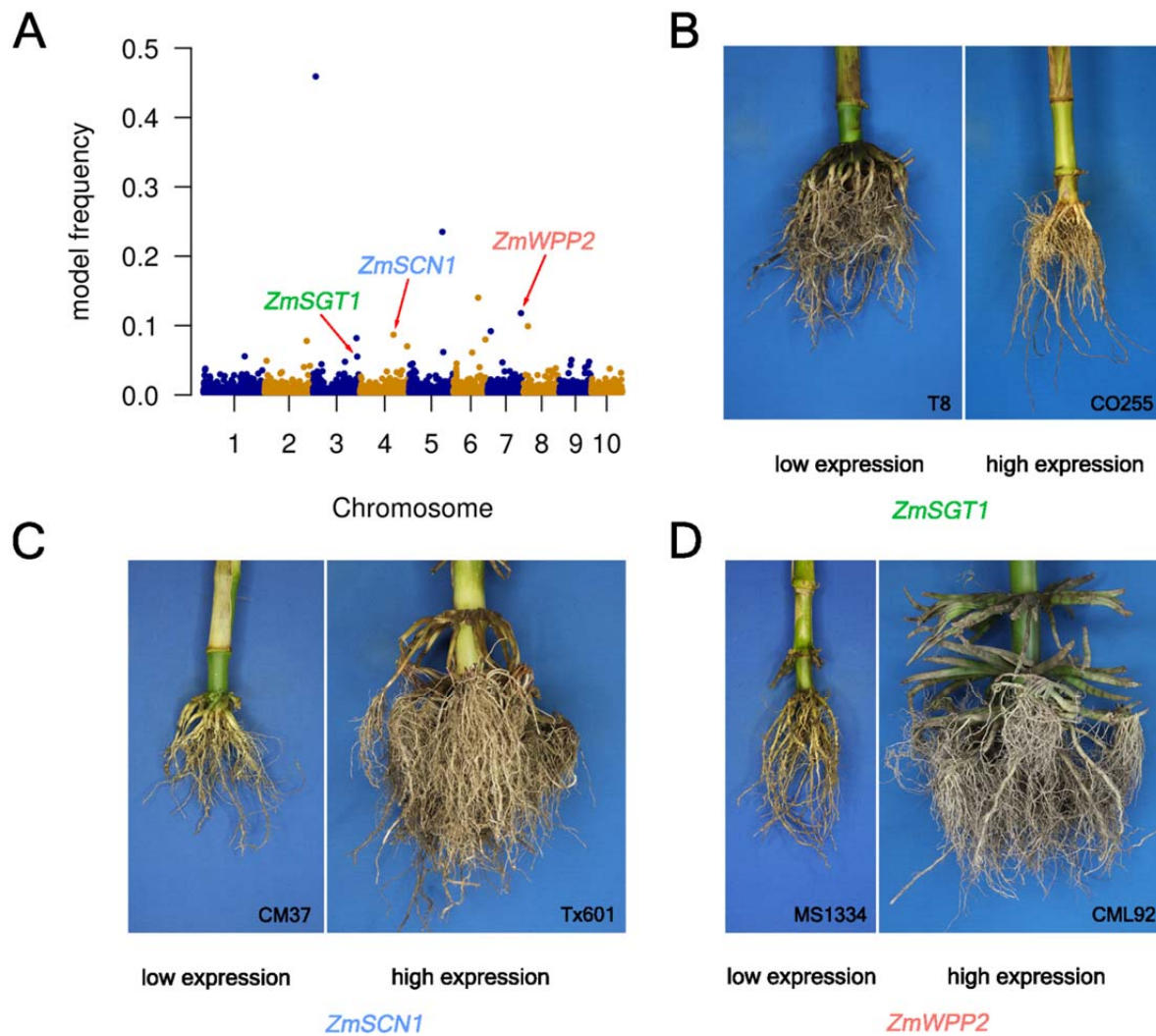


Figure 3: Expression levels of three maize homologs of Arabidopsis root-related genes were associated with *smArea* via eRD-GWAS. A) Manhattan plot of eRD-GWAS for *smArea*. Three homologs of Arabidopsis root-related genes: *ZmSGT1* (GRMZM2G105019), *ZmSCN1* (GRMZM2G012814), and *zmWPP2* (GRMZM2G309970) were detected. Correlation coefficients (r) of expression levels and trait values of *smArea* for the three genes are: -0.23, 0.25 and 0.22, respectively. $P < 0.01$ for all correlations. B-D) Representative root images of inbred lines having extremely low and extremely high expression levels of the three candidate genes.

310 with root development in Arabidopsis. An Arabidopsis mutant, *sgt1b* (a homolog of
 311 GRMZM2G105019), exhibits auxin-resistant root growth under low concentrations of auxin
 312 (Gray et al., 2003). An RNAi mutant of *wpp2* (a homolog of GRMZM2G309970) exhibits
 313 delayed root development, reduced root length, and fewer lateral roots as compared to wild-type
 314 controls (Patel et al., 2004). *SCN1* (a homolog of GRMZM2G012814) encodes a RhoGTPase

315 GDP dissociation inhibitor (RhoGDI) that restricts the initiation of root hairs to trichoblasts
316 (Carol et al., 2005).

317 **Network Analyses of RSA-associated Genes**

318 Expression quantitative trait loci (eQTL) mapping is used to identify DNA polymorphisms
319 associated with variation in gene regulation (Gilad et al., 2008). 110 of the RSA-candidate genes
320 were expressed in at least half of the 246 genotypes used for eRD-GWAS. eQTL analyses were
321 conducted for each of the 66/77 qualified SNP-genes and each of the 44/62 eRD-genes that
322 passed this expression profile criterion (Methods). At an FDR cutoff of < 0.05 , 601 eQTL were
323 identified for 58/66 (88%) of the SNP-genes and 39/44 (89%) of the eRD-genes (Supplemental
324 Table S10). 69/601 (11.5%) and 447/511 (88.5%) of these eQTL acted in *cis* and *trans*,
325 respectively (Supplemental Table S11; Methods). 36 of the 97 (=58+39) (37%) SNP-genes and
326 eRD-genes are themselves *trans*-eQTL for at least one of the other 61 genes. This level of
327 enrichment is statistically significant ($p = 2.2e-16$, Methods), and suggests the existence of a
328 regulatory network involving both SNP-genes and eRD-genes.

329
330 To further explore the existence of a regulatory network, a Gaussian Graphical Model (GGM)
331 was used to construct a GGM-based co-expression network for the 246 genotypes using the
332 RNA-Seq data from root tips that had been used in the eQTL analyses, and thereby identify
333 putative regulatory relationships among the 139 RSA-associated genes (77 SNP-genes and 62
334 eRD-genes) and the nine root-related genes (eight cloned maize root-related genes, plus *rum1*-
335 *like1*, a homeolog of *rum1*) (Hochholdinger et al., 2018) (Methods). In total, 26 unique RSA-
336 associated genes (16/77 SNP-genes and 10/62 eRD-genes) are co-expressed with one or more
337 cloned maize root-related genes. For example, 17 root candidate genes (nine SNP-genes and
338 eight eRD-genes) were included in the GGM-based co-expression network that contains *rth1*,
339 *rum1*, *rull*, and *bige1* (Figure 4). The *rth1* gene encodes the SEC3 subunit (Wen et al., 2005) of
340 the exocyst complex (Hala et al., 2008) that controls the exocytotic growth of root hair tip. The
341 *rum1* gene encodes an AUX/IAA protein and plays key roles in lateral and seminal root
342 formation (Woll et al., 2005; Zhang et al., 2016), whereas *rull* is a homeolog of *rum1* that
343 exhibits 92% sequence identity and shares the canonical features of AUX/IAA protein (Von
344 Behrens et al., 2011). In another module of the GGM-based co-expression network, nine root
345 candidate genes (seven SNP-genes and two eRD-genes) were co-expressed with *rth3*, *rth5*, and

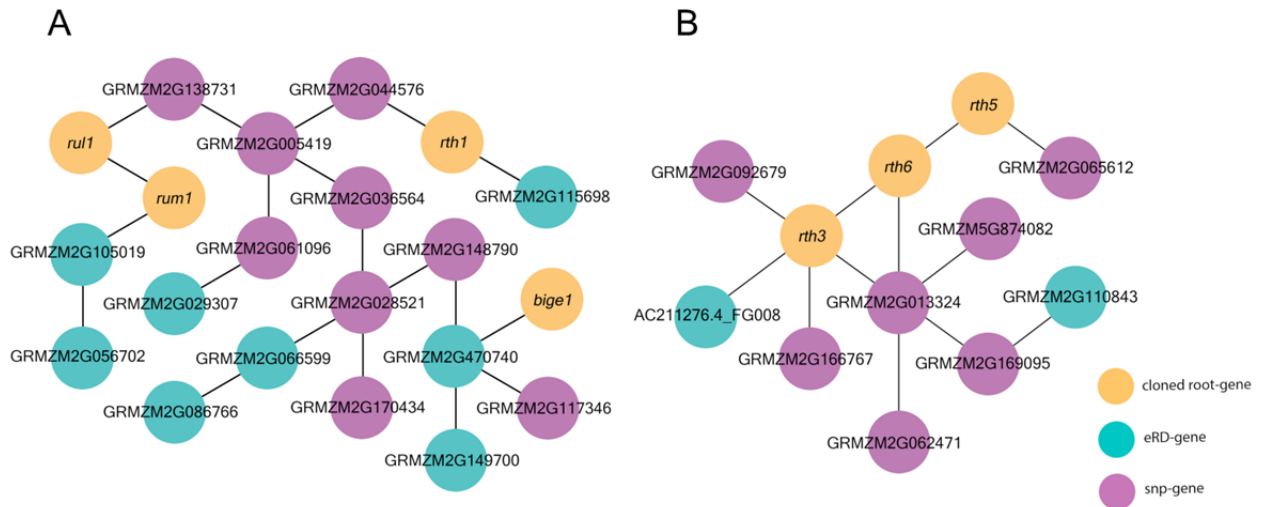


Figure 4: **Gaussian Graphical Model-based co-expression networks.** Two clusters illustrating putative regulatory relationships among RSA-associated genes and cloned root genes. Yellow dots indicate cloned root related genes, green dots indicate genes identified via eRD GWAS, and purple dots indicate genes identified via SNP-based GWAS.

346 *rth6* (Figure 4). *rth5* and *rth6* play important roles in cellulose biosynthesis and are involved in
 347 root hair elongation (Nestler et al., 2014; Li et al., 2016), whereas *rth3* is a member of COBRA
 348 gene family that is required for root hair elongation and contributes to grain yield (Wen &
 349 Schnable, 1994; Hochholdinger et al., 2008).

350

351 **Comparative GWAS for RSA of maize and sorghum**

352 Core root systems of up to five competitive plants were also collected and phenotyped using the
 353 CREAMD-COFE pipeline for a subset (N = 294) of the Sorghum Association Panel (SAP) (Casa
 354 et al., 2008), which will be designated the SAP-RSA (Supplemental Table S12). The SAP-RSA
 355 was grown in Mead, NE (Methods) and phenotyped using CREAMD-COFE for the same RSA
 356 traits as was done for maize. The heritabilities and pair-wise correlations of these traits in
 357 sorghum were similar to maize (Supplemental Figure S8). GWAS for the SAP-RSA was
 358 conducted using 205k SNPs from published GBS data (Morris et al., 2013). In total, 132 TASs
 359 (comprising 115 unique TASs) were detected for the RSA traits with FDR < 0.05 (Supplemental
 360 Table S13). Among the 132 sorghum TASs, 9% (12/132) were associated with multiple RSA
 361 traits or two views of the same RSA trait. Whereas the minor allele frequencies (MAFs) of
 362 sorghum TASs are similar to those of the maize, the effect sizes of TASs, which is an estimate of
 363 the contribution of each SNP to the total genetic variance (Park et al., 2011), from sorghum are

364 significantly larger than those from maize ($p < 0.01$) (Supplemental Figure S9), presumably
365 reflecting the greater statistical power of the maize GWAS, resulting in a greater ability to detect
366 smaller effect loci.

367

368 The similarities of maize and sorghum RSAs (Yamauchi et al., 1987), in addition to the syntenic
369 relationship of their genomes (Schnable et al., 2011; Schnable et al., 2012) led us to hypothesize
370 that these species have conserved genetic control for RSA. To test this hypothesis, a comparison
371 was conducted between the unique TASs from GWAS for RSA for maize and sorghum. Syntenic
372 genes were identified within 20-kb windows centered on maize TASs and 500-kb windows
373 centered on sorghum TASs (Methods). These window sizes were selected based on average LD
374 values of 10 kb and 250 kb for the SAM diversity and SAP-RSA panels, respectively (Methods).
375 Using an FDR cut-off of <0.05 for both species, seven pairs of syntenic genes were identified
376 (Supplemental Table S14). Based on a permutation test, this is more overlap than would be
377 expected by chance ($p = 1e-04$, Methods). For example, GRMZM2G028521, annotated as maize
378 *citrate transporter 1 (citt1)*, was identified via SNP-based GWAS for *smArea* and *IgMaxWidth*.
379 Its sorghum homolog Sb01g047080 was 138 kb away from the sorghum TAS associated with
380 both *smArea* and *IgMaxWidth* (Figure 5). Although some syntenic gene pairs were not associated
381 with the same RSA traits in maize and sorghum, the associated traits exhibited high correlations.

382

383 This is also more overlap than we detected in two pairs of intraspecific GWAS for above-ground
384 traits conducted as controls. First, we conducted GWAS for multiple traits using mostly
385 previously published data from two genetically distinct maize diversity panels grown in separate
386 environments. The Yan panel, which consists of 368 inbred lines, was grown in China (Li et al.,
387 2013; Yang et al., 2014), whereas the SAM Diversity Panel (Leiboff et al., 2015) was grown in
388 the US (Methods). These panels do not include any shared inbred lines. Both panels were
389 phenotyped for four traits: plant height, plant ear height, flowering time, and ear length Data for
390 the Yan and SAM Diversity Panels were obtained from Yang et al. (2014) and Leiboff et al.
391 (2015), respectively (except for EL of the SAM Diversity Panel, which is previously unpublished
392 data, see Methods). Through GWAS conducted using an FDR cutoff of <0.05 for both panels, 24
393 and 18 TASs were detected from the Yan and SAM Diversity Panels, respectively (Supplemental
394 Table S15). Using methodology similar to that described for the comparative *interspecific*

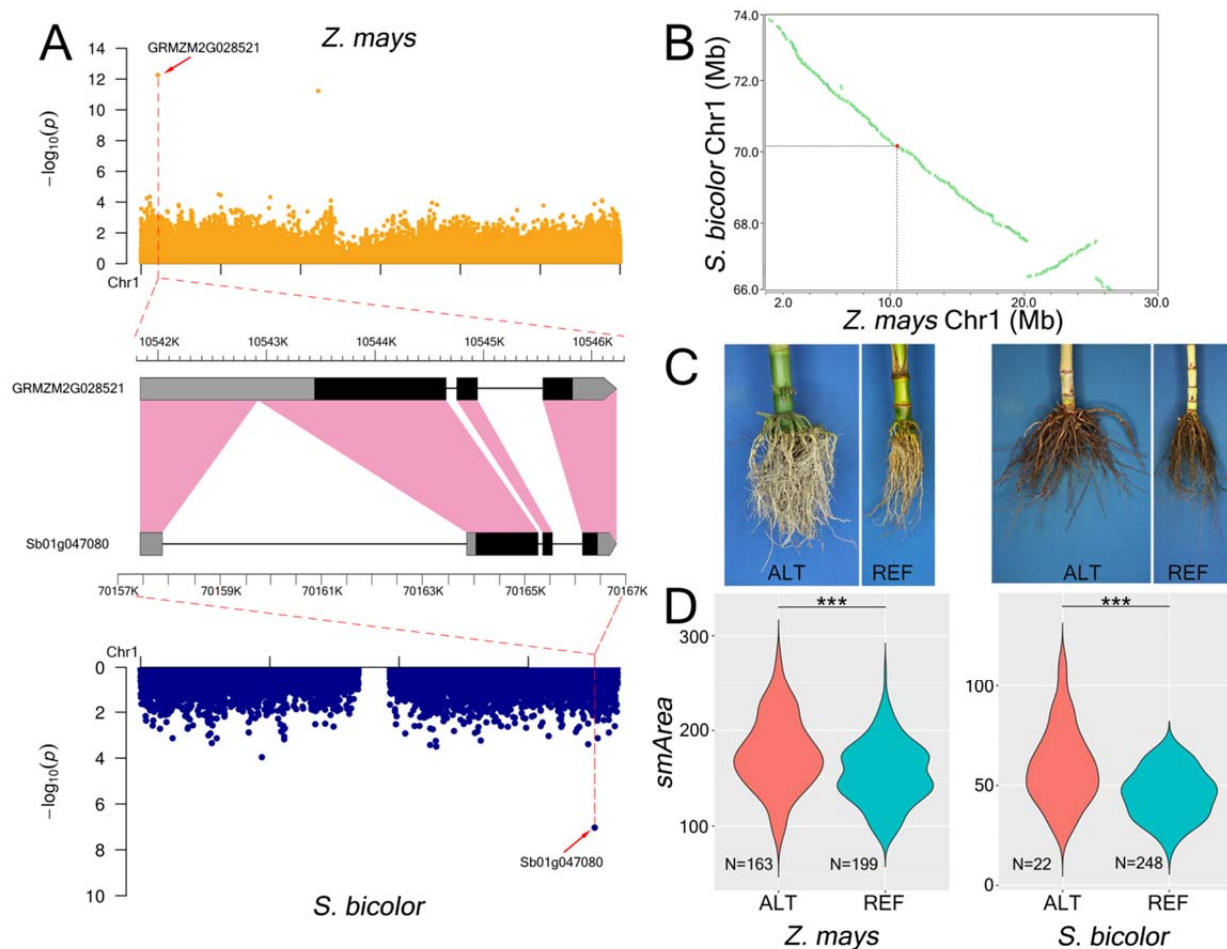


Figure 5: **Comparative GWAS between maize and sorghum for *smArea*.** A) Manhattan plots of Chromosome I from SNP-based GWAS for *smArea* of maize (top) and sorghum (bottom) identified a pair of RSA-associated syntenic genes; homologous sequences are indicated in pink. B. Genomic positions of the syntenic gene pair from panel A. C) Inbred lines of maize (left pair; LH150 and A188) and sorghum (right pair; White Kafir and D940Y) fixed for ALT and REF alleles of the SNPs associated with *smArea*. D) Distribution of trait values of maize (left) and sorghum (right) inbred lines homozygous for the ALT and REF alleles of the SNPs associated with *smArea*. Student's t-test; stars indicate $p < 0.001$.

395 GWAS for RSA (Methods), no overlapping TAs were identified between the two maize panels,
 396 even using window sizes as large as 100 kb. Next, we conducted another pair of *intraspecific*
 397 GWAS on two diversity panels that consisted of the same inbred lines and that were genotyped
 398 with the same set of SNPs, but that were grown in different environments and phenotyped by
 399 different groups. 97% (273/282) of the members of the Maize 282 association panel (Peiffer et
 400 al., 2014) are a subset of the SAM panel. This subset of 273 inbred lines will be referred as the

401 “Maize273” and “SAM273” panels. Both panels were phenotyped for four traits: plant height,
402 plant ear height, flowering time, and ear length (Methods). 15 and 13 TASs were detected from
403 the Maize273 and SAM273 panels, respectively (Supplemental Table S16). Even though
404 presumably genetically identical inbred lines were analyzed with the same genotyping data, only
405 two overlapping TAS were identified. The number of shared candidates did not increase even
406 when using window sizes up to 100 kb. The absence of shared signals identified via GWAS
407 conducted within a single species and the very small number of overlapping signals within a
408 single diversity panel provides further evidence that the multiple pairs of RSA-associated
409 syntenic genes detected between the two species is significant.

410
411
412

413 **Discussion**

414 Accurate phenotyping is an essential component of GWAS. Phenotyping RSA, i.e., the topology
415 and distribution of roots (Lynch, 1995), is challenging due to tradeoffs between throughput and
416 intactness (Topp et al., 2016). To enable high-throughput excavation and cleaning of core root
417 systems, thereby making feasible GWAS for RSA, we developed the CREAMD pipeline, which
418 offers a 6X speed advantage in root cleaning as compared to conventional water-based methods
419 (Trachsel et al., 2011; Colombi et al., 2015), while yielding comparably intact core root systems.
420 In addition, the towable air-compressor, which is the key component of the CREAMD pipeline,
421 simplifies the phenotyping of RSA in multiple environments, even when a nearby water source is
422 not available. This promises to make the study of genotype-environment interactions (GXE) of
423 RSA feasible.

424

425 Another phenotyping challenge is the complicated topology and structure of RSA, particularly of
426 adult plants. Like others (Trachsel et al., 2011; Topp et al., 2013; Pace et al., 2014), we used
427 multiple 2D images in an effort to capture more of the 3D complexity of RSA. To convert these
428 images to trait values we developed the COFE software, which offers several advantages relative
429 to alternative software packages such as GiA Roots (Galkovskyi et al., 2012) and DIRT (Das et
430 al., 2015). The accuracy and flexibility of the CREAMD-COFE pipeline is supported both by
431 comparisons to ground truth data and the relatively high heritabilities observed across highly
432 diverse germplasm that exhibits highly divergent RSA phenotypes. Because the density cutoffs
433 used for the AdjDepth traits were selected to maximize heritabilities (Supplemental Figure S5)
434 and these cut-offs are likely to be affected by factors such as soil type, crop management,
435 excavation date, and weather, we recommend determining the optimal cut-offs for each
436 independent project.

437

438 The availability of the CREAMD-COFE pipeline enabled us to conduct high-throughput
439 phenotyping of RSA traits in diversity panels of adult, field-grown maize and sorghum plants.
440 After collecting phenotypic data, we employed two complementary GWAS approaches to
441 identify RSA-associated maize genes. Conventional SNP-based GWAS associate variation in
442 SNP genotypes across a diversity panel with phenotypic variation. By contrast, eRD-GWAS uses
443 expression levels of genes as the explanatory variable for GWAS (Lin et al., 2017). The

444 robustness of eRD-GWAS is demonstrated by the fact that even though read counts obtained
445 from RNA-seq data from root tips excised from germinating seedlings were used as the
446 explanatory variable for the RSA of adult field-grown plants, it was still possible to identify
447 strongly supported candidate genes. Consistent with Lin et al. (2017), few RSA-associated genes
448 were detected by both GWAS approaches, providing further evidence that the two approaches
449 are complementary.

450
451 The ability of our pipeline to detect true positives is supported by the finding that homologs of
452 16% (22/139) of the RSA-associated maize genes are known to affect RSA in other species, one
453 of the highest confirmation rates reported in crops (Xiao et al., 2017). In addition, 26 RSA-
454 associated genes are co-regulated with genes previously shown to affect RSA and 37% of RSA-
455 associated genes are themselves *trans*-eQTL for at least one other qualified RSA-associated gene
456 (again, significantly more than would be expected by chance). Finally, we detected substantially
457 more pairs of RSA-associated syntenic genes in maize and sorghum than would be expected by
458 chance. In combination, these results provide strong support for the accuracies of our gene/trait
459 associations and demonstrate that the CREAMD-COFE pipeline is sufficiently accurate for use
460 in GWAS.

461
462 We photographed each core root system from two directions. Initially, we were surprised that
463 there was little overlap between the SNPs or genes associated with a given trait from the two
464 views. However, in contrast to published reports (Colombi et al., 2015) we showed that core root
465 systems are not radially symmetrical. As a consequence of this asymmetry, the two 2D images
466 we captured of a given core root system typically exhibited different trait values. It is therefore
467 not surprising that we often identified different genes as being associated with the same nominal
468 “trait” from the smaller and larger views of the same core root system.

469
470 Seven pairs of syntenic maize and sorghum genes are associated with RSA traits, which is
471 significantly more overlap than would be expected by chance. Chen et al. (2016) used a
472 comparative GWAS approach to identify shared genetic control among maize and rice homologs
473 for biochemical composition of grain and leaves. Their analysis relied upon conservation of

474 biochemical pathways across taxa. It was not obvious that the regulation of morphology would
475 be shared across taxa as has been demonstrated by the current study.

476

477 There is substantial overlap among the RSA-associated genes detected in maize and sorghum
478 that were grown in different environments but phenotyped by the same group using the same
479 methodology. This is in line with the observation that overall gene expression profiles of maize
480 roots are substantially more influenced by genotype than by environmental stress factors such as
481 drought (Marcon *et al.*, 2017). By contrast, we found no overlap among trait-associated genes
482 from the same panel of maize inbred lines that had been genotyped with the same markers, but
483 were grown in different environments and phenotyped by different groups. Although these two
484 groups were nominally measuring the same traits, the lack of overlap among trait-associated
485 genes suggests that differences in phenotyping methodologies and hence trait values may be a
486 major contributor to differences in GWAS results among experiments.

487

488 Given its fast rate of LD decay, GWAS in maize results in single-gene or near single-gene
489 resolution. By contrast, as a consequence of its slower rate LD decay as compared to maize
490 (Morris *et al.*, 2013), GWAS in sorghum does not (Li *et al.*, 2015). However, due to the syntenic
491 relationship between maize and sorghum (Schnable *et al.*, 2011; Schnable *et al.*, 2012), our data
492 indicate that GWAS in maize has the potential to identify candidate genes in that control
493 quantitative traits within large chromosomal windows of sorghum.

494

495 More generally, our results suggest that comparative multi-species GWAS has the potential to
496 enhance our understanding of within-species genetic architecture. Indeed, some RSA-associated
497 genes detected in maize but not sorghum may be false-negative associations (and vice-versa).
498 This is because within a given species it may not be possible to detect an association between a
499 gene and a relevant trait as a consequence of (among other factors) low minor allele frequencies,
500 small effect sizes and/or evolutionary histories (Lai *et al.*, 2018). Hence, just as phenotypes of
501 qualitative mutants identified in one species can inform our understanding of gene function in
502 related species (Lin *et al.*, 2012; Huang *et al.*, 2017; Wang *et al.*, 2018), GWAS results from one
503 species have the potential to identify candidate genes in related species that are not detectable via
504 single-species GWAS.

505
506
507
508
509
510
511
512
513
514
515
516
517
518
519
520
521
522
523
524
525
526
527
528
529
530
531
532
533
534
535
536

Conclusion

We report on a high-throughput phenotyping pipeline that uses compressed air to harvest and clean roots, thereby overcoming current throughput limitations. We used this approach to phenotype RSA in both maize and sorghum diversity panels and then conducted GWAS. The finding that homologs of 16% (22/139) of the detected RSA-associated maize genes are known to affect RSA in other species (one of the highest confirmation rates reported in any crop) demonstrates the accuracy of our phenotyping and analysis pipeline and suggests that the RSA-associated genes detected in this study are worthy of further investigation and exploration for use in crop improvement. Comparisons between high-confidence, RSA-associated genes identified from maize and sorghum via GWAS revealed conserved functional roles of syntenic orthologs in regulating quantitative variation. Our findings suggest that GWAS results from one species have the potential to identify candidate genes in related species that are not detectable in that second species as a consequence of, for example, low minor allele frequencies, small effect sizes, and/or differing evolutionary histories.

Materials and Methods

Germplasm for GWAS

Three fully randomized replications of 380 maize (*Zea mays*) inbred lines were grown at the Iowa State University's Curtiss Research Farm in Ames, IA with a planting date of May 9th 2017 and an inter-row spacing of 88.9 cm and an average within row plant-to-plant spacing of 25.4 cm. Only phenotypic data from the 369 lines in the SAM Diversity Panel (Leiboff et al., 2015) were used for GWAS.

For sorghum (*Sorghum bicolor*), a subset of the Sorghum Association Panel (SAP) (Casa et al., 2008) was grown at the Agronomy Farm of University of Nebraska-Lincoln (UNL), Mead, NE with a planting date of May 15th 2017 and a planting density an interrow spacing of 72 cm and an average within row plant-to-plant spacing of 7.7 cm. Phenotypic data from 294 accessions of the SAP, referred to as the SAP-RSA, were used for GWAS.

537 **CREAMD - Collection and Phenotyping of Core Root Systems**

538 Core root systems, each with approximately 0.3-m³ volume (Hauck et al., 2015), of typically
539 three competitive plants (i.e., plants that are not the terminal plant at the beginning or end of a
540 row nor adjacent to a missing plant within a row) within a row were excavated and cleaned on
541 site using a towable commercial air compressor and an AirSpade[®] device (Supplemental Text
542 S2). Up to three maize roots were collected from up to three biological replications (i.e. plants
543 grow in three different one-row plots) for a total of up to nine roots per genotype. Roots of each
544 genotype were collected within one week of the end of flowering for that genotype. For the SAP-
545 RSA, typically five competitive sorghum plants within each row were excavated and cleaned
546 between October 12th and 18th (2017) following the same protocol. In most cases for both species
547 it was possible to harvest competitive plants. Harvested plants that were non-competitive (i.e.,
548 adjacent to a missing plant, or that were a border plant) or that had lodged were recorded for
549 subsequent statistical modeling (see below).

550
551 Cleaned core root systems were imaged on a customized board (40.6 cm x 50.8 cm) covered with
552 blue fabric. Core root systems were positioned on the center of the imaging board and a
553 dimmable 45.7 cm-diameter light ring (Neewer Technology Co., Shenzhen, China) was placed
554 directly beneath the camera lens to provide evenly distributed lighting to reduce shadows. A
555 round orange marker ($\varnothing = 5.1$ cm) and a tag containing an ID number for each plant were placed
556 on the imaging platform next to the corresponding core root system. All images were captured
557 using an EOS 5D Mark III with an EF 24-105 mm f/4L IS USM lens (Canon, Tokyo, Japan),
558 positioned 125 cm above the imaging board surface using an adjustable mount. The camera was
559 controlled using a laptop computer (Latitude 3550, Dell, Round Rock, USA) running EOS
560 Utility 3 software (Version 3.6.30.0) to capture images. Two images from two orthogonal views
561 (North and West) of the core root system were taken based on the spray-painted identifier.
562 Images were stored using JPEG file format.

563
564 For both the maize and sorghum diversity panels, a random 5% of all collected core root systems
565 (149 maize roots and 56 sorghum roots) were chosen for ground truth measurement. The
566 maximum width and depth of core root system were manually measured for both of the two

567 orthogonal views (Supplemental Figure S2). In addition, ImageJ (Schneider et al., 2012) was
568 used to measure maximum width and depth from the images of the same sets of roots.

569
570 To determine whether core root systems exhibit radial symmetry, we collected four to six plants
571 of the inbred lines B73 and Mo17 from three locations near Ames, IA on September 23rd 2018:
572 Curtiss Farm (GPS: 42°00'N, 93°39'W, planting date: May 31st 2018, planting density:
573 ~36 cm within row, 3 m between rows), Marsden Farm (GPS: 42°00'N, 93°47'W, planting date:
574 May 23rd 2018, planting density: ~36 cm within row, 3 m between rows) and South Woodruff
575 Farm (GPS: 41°58'N, 93°41'W, planting date: June 15th 2018; planting density: ~25 cm within
576 row, 75 cm between rows) (Supplemental Figure S3).

577

578 **COFE - Image Analysis and feature extraction**

579 For image analysis, we used MATLAB (The Mathworks, Natick Massachusetts, USA) to
580 develop an interactive software, Core Root Feature Extraction (COFE). Captured images were
581 analyzed via a two-phase process: pre-processing and trait extraction (Supplemental Text S1).
582 During pre-processing, the first visible node above the soil line of a core root system is identified
583 by the user. Then, the software automatically generates a binary image of the root according to
584 user-defined settings. During automated trait extraction the software uses a blurring and
585 thresholding algorithm to prune roots that aberrantly stick out from the core root system and then
586 extracts traits from the core root system.

587

588 **Comparison of CREAMD vs. Water-based Root Cleaning**

589 The inbred lines B73, LH185, and PHN46 and the commercial hybrid Hoegemeyer 7089, grown
590 during the summer of 2017 at the Curtiss Farm, were used to compare CREAMD vs. a water-
591 based root cleaning pipeline (Trachsel et al., 2011). For each method, 15 competitive plants of
592 each genotype were processed at the time of grain harvest on October 24th 2017. The cleaning of
593 roots with pressurized air is described in the CREAMD protocol (Methods, Notes S1). For the
594 water-based root cleaning, the excavated core root system was soaked in water for ~1 hour and
595 then water washed as described (Trachsel et al., 2011; Colombi et al., 2015). Traits were
596 extracted using COFE from images of core root systems excavated and cleaned by both methods.

597

598 **Comparative GWAS between Maize and Sorghum**

599 For the analysis of maize RSA phenotypes, the best linear unbiased prediction (BLUP) of traits
600 extracted from COFE were calculated by treating genotype and planting row as random effects,
601 and lodging and border status as fixed effects using R package ‘lme4’ v1.1-21 (Bates et al., 2015)
602 (Supplemental Table S17). Broad sense heritability was calculated for all RSA traits for both
603 maize and sorghum (Cai et al. 2012). For the analysis of sorghum RSA phenotypes, means of
604 extracted trait values of all plants having the same genotype were calculated, after removing
605 extreme values, i.e., those that were 1.5X larger than the 3rd quartile (Supplemental Table S18).

606
607 To conduct GWAS on the maize SAM diversity and sorghum SAP-RSA panels, we used 1.2M
608 (Leiboff et al., 2015) and 205k (Morris et al., 2013) SNPs, respectively, without filtering for
609 MAF (Bomba et al., 2017). GWAS for both species were conducted using a C++ implementation
610 of FarmCPU (Liu et al., 2016), termed FarmCPUpp (Kusmec and Schnable, 2018). Based on
611 simulation studies, for moderately complex traits, FarmCPU has been reported to have the best
612 metrics for both the detection of gene-trait associations and false-positive metrics (Miao et al.,
613 2018). The first three principle components calculated using TASSEL 5.0 were used as
614 covariates to control for population structure (Bradbury et al., 2007). Linkage disequilibrium
615 (LD) values of both panels were calculated using PLINK v1.90 (Purcell et al., 2007). Based on
616 the average rates of LD in the diversity panels, 20- and 500-kb windows centered on TASs were
617 used to identify candidate genes in maize and sorghum, respectively. Maize AGPv2 genes
618 models (Schnable et al., 2009) and sorghum V1.14 genes models (Paterson et al., 2009) that
619 overlapped with the defined windows for each species using the BEDtools software (Quinlan and
620 Hall, 2010) (V2.23.0) were considered to be candidate genes.

621
622 In addition to SNP-based GWAS, eRD-GWAS (Lin et al., 2017) was conducted on a subset of
623 the SAM Diversity Panel (N=246 inbred lines) for which RNA-Seq data from seedling root
624 tissue were available (Kremling et al., 2018). Genes with model frequencies over an arbitrary
625 cutoff of 0.05 were designated as candidate genes (eRD-genes).

626
627 Maize and sorghum syntenic genes were identified following the methods of Zhang et al. (2017)
628 using the reference genomes RefGen V2 for maize and Sbi1.4 for sorghum (Supplemental Table

629 S19). The permutation test was conducted by shuffling the maize-sorghum table 10,000 times
630 and counting the number of pairs of syntenic genes obtained from each trial (Supplemental Table
631 S19)

632

633 **eQTL and co-expression network**

634 eQTL analyses were conducted on the same 246 maize inbred lines as were used for eRD-
635 GWAS, and using the same GWAS method (i.e., FarmCPU) and SNPs as were used for the
636 maize RSA GWAS (see above), with the gene expression values as phenotypes and the SNPs as
637 explanatory variables. Only those maize RSA candidate genes expressed in at least 50% of the
638 246 lines were included in this analysis. An eQTL was defined as acting in *cis* if it was within a
639 window that extends 500 kb upstream and 500 kb downstream of the gene it regulates; eQTL
640 outside this 1-Mb window were defined as acting in *trans*. Ratios of *cis*- and *trans*-eQTL were
641 relatively stable with window sizes ranging from 50 kb–2 Mb (Supplemental Table S10). The
642 eQTL with the smallest p-value within each 50-kb window was selected for further analyses. The
643 enrichment test of RSA-associated genes and *trans*-eQTL was performed using the “fisher.test ()”
644 function in R.

645

646 Graphical Gaussian Model-based co-expression networks were constructed using the R package
647 ‘bnlearn’ v4.4.1 (Scutari, 2010) with 5,000 bootstraps implemented with the constraint-based
648 learning algorithm max-min parents and children (mmpc).

649

650 **Comparative intraspecific GWAS**

651 Both phenotypic and genotypic data of the Yan panel were retrieved from MaizeGo
652 (<http://www.maizego.org/Resources.html>). SNP data for the Yan panel were generated by Li et
653 al. (2013) from RNA-Seq and MaizeSNP50 BeadChip. Phenotypic data of the Maize 282 panel
654 were retrieved from Panzea
655 (<http://cbsusrv04.tc.cornell.edu/users/panzea/filegateway.aspx?category=Phenotypes>).

656 Phenotypic data of plant height, plant ear height, and flowering time of the SAM Diversity Panel
657 were from Leiboff et al. (2015). Ear length data were collected from two fully randomized
658 replications of 369 maize inbred lines from the SAM Diversity Panel (Leiboff et al., 2015) in
659 October 2016, at Iowa State University’s Curtiss Research Farm (42°00’N, 93°39’W) in Ames,

660 IA, USA (Supplemental Table S20). Genotypic data for both the Maize273 and SAM273 panels
661 is a subset of the data used for the root-GWAS of the SAM Diversity Panel. GWAS was
662 conducted with the same protocol as in comparative GWAS between maize and sorghum (see
663 above section), except an arbitrarily relaxed window of 100 kb, centered on the TAS was used
664 here.

665

666 **COFE Software availability:** <https://bitbucket.org/baskargroup/cofe/src/master/>

667

668 **Accession Numbers**

669 The maize sequence data from this article can be found in the GenBank/EMBL data libraries
670 under accession numbers SRP055871. The sorghum SNP data was downloaded from
671 <https://www.morrislab.org/data>.

672

673 .

674

675

676 **Supplemental Data**

677

678 **Supplemental Text S1.** CREAMD-COFE protocols

679 **Supplemental Text S2.** Definition of Width-Profile Angle (WPA)

680 **Supplemental Figure S1.** Ground truth validation for trait values extracted from COFE. 298

681 images from 149 maize plants were analyzed.

682 **Supplemental Figure S2.** Comparisons of trait values extracted using COFE from roots of three
683 genotypes.

684 **Supplemental Figure S3.** Maize core root systems grown in three environments (Curtiss,
685 Marsden, and South Woodruff farms) exhibit a lack of radial symmetry.

686 **Supplemental Figure S4.** Classification of images taken from two angles (North and West) into
687 larger and smaller view on a *per trait* basis.

688 **Supplemental Figure S5.** Illustration of algorithm for determining root depth (AdjDepth) trait
689 values

690 **Supplemental Figure S6.** Width-Profile Angle (WPA) was used to measure root angle.

691 **Supplemental Figure S7.** Above-ground trait values of inbred lines homozygous for the ALT
692 and REF alleles of bige1.

693 **Supplemental Figure S8.** Correlations among RSA traits for 294 sorghum inbred lines.

694 **Supplemental Figure S9.** Minor allele frequency (MAF) and the absolute value of effect sizes
695 of maize and sorghum TAS.

696 **Supplemental Table S1.** Time required to process 60 core root systems via CREAMD and
697 water-based root cleaning.

698 **Supplemental Table S2.** RSA traits do not exhibit statistically different values between two
699 orthogonal views (North and West) of the maize SAM Diversity Panel.

700 **Supplemental Table S3.** Classification of trait values of root area (Area) from two angles
701 (North and West) into larger and smaller views on a *per trait* basis.

702 **Supplemental Table S4.** Correlation coefficients between larger and smaller views of RSA
703 traits in the maize SAM diversity and sorghum (SAP-RSA) panels.

704 **Supplemental Table S5.** Correlations among RSA traits and above-ground traits in maize.

705 **Supplemental Table S6.** Maize TAS and SNP-genes at FDR < 0.05

706 **Supplemental Table S7.** Arabidopsis homologs with known root-related functions of maize
707 SNP-genes

708 **Supplemental Table S8.** List of eRD-genes

709 **Supplemental Table S9.** Arabidopsis and Medicago homologs with known root-related
710 functions of maize eRD-genes.

711 **Supplemental Table S10.** List of cis- and trans-eQTL.

712 **Supplemental Table S11.** Percentage of cis- and trans-eQTL for qualified maize RSA-
713 associated genes using different window sizes

714 **Supplemental Table S12.** List of inbred lines in used in GWAS for maize (SAM Diversity
715 Panel) and sorghum (SAP-RSA)

716 **Supplemental Table S13.** Sorghum TAS at FDR < 0.05

717 **Supplemental Table S14.** Syntenic maize-sorghum gene pairs detected via comparative GWAS.

718 **Supplemental Table S15.** List of Yan panel and SAM Diversity Panel TAS for four traits (PH,
719 PEH, DTA, EL)

720 **Supplemental Table S16.** List of TAS for four traits (PH, PEH, DTA, EL) identified via GWAS
721 conducted on the maize₂₇₃ and SAM₂₇₃ panels.

722 **Supplemental Table S17.** RSA trait values (BLUP) of maize SAM Diversity Panel.

723 **Supplemental Table S18.** RSA trait values of sorghum SAP-RSA panel.

724 **Supplemental Table S19.** List of syntenic genes.

725 **Supplemental Table S20.** Ear length trait values (BLUP) of maize SAM Diversity Panel.

726

727

728

729 **Acknowledgments**

730

731 We thank Dr. Dan Nettleton (Iowa State University) for statistical consultation; Cheng-Ting
732 “Eddy” Yeh (P. Schnable Lab) for bioinformatics support; Aaron Kusmec, Hung-Ying Lin,
733 Qiang Liu, and Yan Zhou (graduate students in the P. Schnable Lab) for useful discussions;
734 Colton McNinch (a former graduate student in the P. Schnable Lab) for early testing of the
735 AirSpade® and software; Dr. Melinda Yerka (University of Nevada, Reno) for designing the
736 sorghum field layout; Maureen Booth, Daniel Russell, Leo Savage, Cameron Lahn, Trenton
737 Houston (undergraduate research assistants in the P. Schnable Lab), and Tyler Greenwald
738 (undergraduate research assistant at the University of Nebraska, Lincoln) for assisting with root
739 collection and/or phenotyping; and Drs. Lakshmi Attigala and An-Ping Hsia (P. Schnable Lab)
740 for assistance editing the manuscript.

741

742

743

744 **Table**

745

746 Table 1. Abbreviations of RSA traits.

747

Abbreviation	Trait
Area	Root Area
ConArea	Convex Hull Area
MedWidth	Median Width
MaxWidth	Maximum Width
WPA	Width-Profile Angle
AdjDepth	Adjusted Depth

748

749

750

751

752

753 **Figure Legends**

754

755 **Figure 1: Extraction of RSA traits from binary images of core root systems using COFE.** A)
756 Illustration of root cleaning and B) phenotyping of CREAMD pipeline; C) Illustration of four out
757 of six traits extracted via COFE; D) Comparison of RSA trait values from the inbred line B73
758 extracted by COFE from roots collected using CREAMD or water-based root cleaning. Data are
759 means \pm SD; ns: not significant, Student's *t*-test; n=15; E) Heritabilities of RSA trait values
760 obtained from the SAM Diversity Panel via CREAMD-COFE; n=3,196 roots per view.

761
762 **Figure 2: Association of *Bige1* (GRMZM2G148937) with maize *smWPA*.** A) Manhattan plot
763 of SNP-based GWAS for *smWPA*; Gene model with the position indicated of the RSA-
764 associated SNP within the intron; B) Representative root images of inbred lines homozygous for
765 the ALT (non-B73) and REF (B73) alleles of the RSA-associated SNP within *Bige1*. Illustrated
766 inbred lines are LH52 (ALT allele) and LH57 (REF allele). C) Distribution of trait values of
767 inbred lines homozygous for the ALT and REF alleles. Student's *t*-test; *** $p < 0.001$.

768
769 **Figure 3: Expression levels of three maize homologs of Arabidopsis root-related genes were**
770 **associated with *smArea* via eRD-GWAS.** A) Manhattan plot of eRD-GWAS for *smArea*. Three
771 homologs of Arabidopsis root-related genes: *ZmSGT1* (GRMZM2G105019), *ZmSCN1*
772 (GRMZM2G012814), and *zmWPP2* (GRMZM2G309970) were detected. Correlation
773 coefficients (r) of expression levels and trait values of *smArea* for the three genes are: -0.23,
774 0.25, and 0.22, respectively. $P < 0.01$ for all correlations. B-D) Representative root images of
775 inbred lines having extremely low and extremely high expression levels of the three candidate
776 genes.

777
778 **Figure 4: Gaussian Graphical Model-based co-expression networks.** Two clusters illustrating
779 putative regulatory relationships among RSA-associated genes (Panel A) and cloned root genes
780 (Panel B). Yellow dots indicate cloned root related genes, green dots indicate genes identified via
781 eRD GWAS, and purple dots indicate genes identified via SNP-based GWAS.

782
783 **Figure 5: Comparative GWAS between maize and sorghum for *smArea*.** A) Manhattan plots
784 of Chromosome 1 from SNP-based GWAS for *smArea* of maize (top) and sorghum (bottom)
785 identified a pair of RSA-associated syntentic genes; homologous sequences are indicated in pink.

786 B) Genomic positions of the syntenic gene pair from panel A. C) Inbred lines of maize (left pair;
787 LH150 and A188) and sorghum (right pair; White Kafir and D940Y) fixed for ALT and REF
788 alleles of the SNPs associated with *smArea*. D) Distribution of trait values of maize (left) and
789 sorghum (right) inbred lines homozygous for the ALT and REF alleles of the SNPs associated
790 with *smArea*. Student's *t*-test; *** $p < 0.001$.

791
792
793
794
795
796
797
798
799
800
801

Parsed Citations

Airoldi CA, Rovere FD, Falasca G, Marino G, Kooiker M, Altamura MM, Citterio S, Kater MM (2010) The Arabidopsis BET Bromodomain Factor GTE4 Is Involved in Maintenance of the Mitotic Cell Cycle during Plant Development. *Plant Physiol* 152: 1320–1334

Pubmed: [Author and Title](#)

Google Scholar: [Author Only](#) [Title Only](#) [Author and Title](#)

Amos B, Walters DT (2006) Maize Root Biomass and Net Rhizodeposited Carbon. *Soil Sci Soc Am J* 70: 1489

Pubmed: [Author and Title](#)

Google Scholar: [Author Only](#) [Title Only](#) [Author and Title](#)

Atkinson JA, Wingen LU, Griffiths M, Pound MP, Gaju O, Foulkes MJ, Le Gouis J, Griffiths S, Bennett MJ, King J, et al (2015) Phenotyping pipeline reveals major seedling root growth QTL in hexaploid wheat. *J Exp Bot* 66: 2283–2292

Pubmed: [Author and Title](#)

Google Scholar: [Author Only](#) [Title Only](#) [Author and Title](#)

Bates D, Mächler M, Bolker B, Walker S (2015) Fitting linear mixed-effects models using lme4. *J Stat Softw.* doi: 10.18637/jss.v067.i01

Pubmed: [Author and Title](#)

Google Scholar: [Author Only](#) [Title Only](#) [Author and Title](#)

Benjamini Y, Hochberg Y (1995) Controlling the false discovery rate: a practical and powerful approach to multiple testing. *J R Stat Soc Ser B* 57: 289–300

Pubmed: [Author and Title](#)

Google Scholar: [Author Only](#) [Title Only](#) [Author and Title](#)

Birnbaum K, Shasha DE, Wang JY, Jung JW, Lambert GM, Galbraith DW, Benfey PN (2003) A Gene Expression Map of the Arabidopsis Root. *Science (80-)* 302: 1956–1961

Pubmed: [Author and Title](#)

Google Scholar: [Author Only](#) [Title Only](#) [Author and Title](#)

Bomba L, Walter K, Soranzo N (2017) The impact of rare and low-frequency genetic variants in common disease. *Genome Biol* 18: 77

Pubmed: [Author and Title](#)

Google Scholar: [Author Only](#) [Title Only](#) [Author and Title](#)

Bradbury PJ, Zhang Z, Kroon DE, Casstevens TM, Ramdoss Y, Buckler ES (2007) TASSEL: Software for association mapping of complex traits in diverse samples. *Bioinformatics* 23: 2633–2635

Pubmed: [Author and Title](#)

Google Scholar: [Author Only](#) [Title Only](#) [Author and Title](#)

Bray JR, Lawrence DB, Pearson LC (2006) Primary Production in Some Minnesota terrestrial Communities for 1957. *Oikos.* doi: 10.2307/3564905

Pubmed: [Author and Title](#)

Google Scholar: [Author Only](#) [Title Only](#) [Author and Title](#)

Cai H, Chen F, Mi G, Zhang F, Maurer HP, Liu W, Reif JC, Yuan L (2012) Mapping QTLs for root system architecture of maize (*Zea mays* L.) in the field at different developmental stages. *Theor Appl Genet* 125: 1313–1324

Pubmed: [Author and Title](#)

Google Scholar: [Author Only](#) [Title Only](#) [Author and Title](#)

Carol RJ, Takeda S, Linstead P, Durrant MC, Kakesova H, Derbyshire P, Drea S, Zarsky V, Dolan L (2005) A RhoGDP dissociation inhibitor spatially regulates growth in root hair cells. *Nature* 438: 1013–1016

Pubmed: [Author and Title](#)

Google Scholar: [Author Only](#) [Title Only](#) [Author and Title](#)

Casa AM, Pressoir G, Brown PJ, Mitchell SE, Rooney WL, Tuinstra MR, Franks CD, Kresovich S (2008) Community resources and strategies for association mapping in Sorghum. *Crop Sci* 48: 30–40

Pubmed: [Author and Title](#)

Google Scholar: [Author Only](#) [Title Only](#) [Author and Title](#)

Chen W, Wang W, Peng M, Gong L, Gao Y, Wan J, Wang S, Shi L, Zhou B, Li Z, et al (2016) Comparative and parallel genome-wide association studies for metabolic and agronomic traits in cereals. *Nat Commun* 7: 1–10

Pubmed: [Author and Title](#)

Google Scholar: [Author Only](#) [Title Only](#) [Author and Title](#)

Colombi T, Kirchgessner N, Le Marié CA, York LM, Lynch JP, Hund A (2015) Next generation shovelomics: set up a tent and REST. *Plant Soil* 388: 1–20

Pubmed: [Author and Title](#)

Google Scholar: [Author Only](#) [Title Only](#) [Author and Title](#)

Courtois B, Audebert A, Dardou A, Roques S, Ghneim-Herrera T, Droc G, Frouin J, Rouan L, Gozé E, Kilian A, et al (2013) Genome-wide association mapping of root traits in a japonica rice panel. *PLoS One* 8: 1–18

Pubmed: [Author and Title](#)

Google Scholar: [Author Only](#) [Title Only](#) [Author and Title](#)

Das A, Schneider H, Burrige J, Ascanio AKM, Wojciechowski T, Topp CN, Lynch JP, Weitz JS, Bucksch A (2015) Digital imaging of root traits (DIRT): A high-throughput computing and collaboration platform for field-based root phenomics. *Plant Methods* 11: 1–12

Pubmed: [Author and Title](#)

Google Scholar: [Author Only](#) [Title Only](#) [Author and Title](#)

Davidson RM, Gowda M, Moghe G, Lin H, Vaillancourt B, Shiu SH, Jiang N, Robin Buell C (2012) Comparative transcriptomics of three Poaceae species reveals patterns of gene expression evolution. *Plant J* 71: 492–502

Pubmed: [Author and Title](#)

Google Scholar: [Author Only](#) [Title Only](#) [Author and Title](#)

Dewey CN (2011) Positional orthology: Putting genomic evolutionary relationships into context. *Brief Bioinform* 12: 401–412

Pubmed: [Author and Title](#)

Google Scholar: [Author Only](#) [Title Only](#) [Author and Title](#)

Dolan L, Janmaat K, Willemssen V, Linstead P, Poethig S, Roberts K, Scheres B (1993) Cellular organisation of the Arabidopsis thaliana root. *Development* 119: 71–84

Pubmed: [Author and Title](#)

Google Scholar: [Author Only](#) [Title Only](#) [Author and Title](#)

Fang S, Yan X, Liao H (2009) 3D reconstruction and dynamic modeling of root architecture in situ and its application to crop phosphorus research. *Plant J* 60: 1096–1108

Pubmed: [Author and Title](#)

Google Scholar: [Author Only](#) [Title Only](#) [Author and Title](#)

Galkovskiy T, Mileyko Y, Bucksch A, Moore B, Symonova O, Price CA, Topp CN, Iyer-pascuzzi AS, Zurek PR, Fang S, et al (2012) GiA Roots : software for the high throughput analysis of plant root system architecture. *BMC Plant Biol* 12: 116

Pubmed: [Author and Title](#)

Google Scholar: [Author Only](#) [Title Only](#) [Author and Title](#)

Gilad Y, Rifkin SA, Pritchard JK (2008) Revealing the architecture of gene regulation: the promise of eQTL studies. *Trends Genet.* doi: 10.1016/j.tig.2008.06.001

Pubmed: [Author and Title](#)

Google Scholar: [Author Only](#) [Title Only](#) [Author and Title](#)

Giuliani S, Sanguineti MC, Tuberosa R, Bellotti M, Salvi S, Landi P (2005) Root-ABA1, a major constitutive QTL, affects maize root architecture and leaf ABA concentration at different water regimes. *J Exp Bot* 56: 3061–3070

Pubmed: [Author and Title](#)

Google Scholar: [Author Only](#) [Title Only](#) [Author and Title](#)

Gray WM, Muskett PR, Chuang H-W, Parker JE (2003) Arabidopsis SGT1b Is Required for SCF TIR1 -Mediated Auxin Response. *Plant Cell* 15: 1310–1319

Pubmed: [Author and Title](#)

Google Scholar: [Author Only](#) [Title Only](#) [Author and Title](#)

Griff TE, Novais J, Bohn M (2011) High-throughput phenotyping technology for maize roots. *Biosyst Eng.* doi: 10.1016/j.biosystemseng.2011.06.004

Pubmed: [Author and Title](#)

Google Scholar: [Author Only](#) [Title Only](#) [Author and Title](#)

Guo J, Chen L, Li Y, Shi Y, Song Y, Zhang D, Li Y, Wang T, Yang D, Li C (2018) Meta-QTL analysis and identification of candidate genes related to root traits in maize. *Euphytica* 214: 223

Pubmed: [Author and Title](#)

Google Scholar: [Author Only](#) [Title Only](#) [Author and Title](#)

Hala M, Cole R, Synek L, Drdova E, Pecenkova T, Nordheim A, Lamkemeyer T, Madlung J, Hochholdinger F, Fowler JE, et al (2008) An Exocyst Complex Functions in Plant Cell Growth in Arabidopsis and Tobacco. *Plant Cell* 20: 1330–1345

Pubmed: [Author and Title](#)

Google Scholar: [Author Only](#) [Title Only](#) [Author and Title](#)

Hargreaves CE, Gregory PJ, Bengough AG (2009) Measuring root traits in barley (*Hordeum vulgare* ssp. *vulgare* and ssp. *spontaneum*) seedlings using gel chambers, soil sacs and X-ray microtomography. *Plant Soil* 316: 285–297

Pubmed: [Author and Title](#)

Google Scholar: [Author Only](#) [Title Only](#) [Author and Title](#)

Hauk AL, Novais J, Griff TE, Bohn MO (2015) Characterization of mature maize (*Zea mays* L.) root system architecture and complexity in a diverse set of Ex-PVP inbreds and hybrids. *Springerplus* 4: 424

Pubmed: [Author and Title](#)

Google Scholar: [Author Only](#) [Title Only](#) [Author and Title](#)

Hochholdinger F, Tuberosa R (2009) Genetic and genomic dissection of maize root development and architecture. *Curr Opin Plant Biol* 12: 172–177

Pubmed: [Author and Title](#)

Google Scholar: [Author Only](#) [Title Only](#) [Author and Title](#)

Hochholdinger F, Wen TJ, Zimmermann R, Ghimot Marcelle P, Da Costa E, Silva O, Bruce W, Lamsey KB, Wienand U, Schnable PS (2008)

The maize (*Zea mays* L.) roothairless3 gene encodes a putative GPI-anchored, monocot-specific, COBRA-like protein that significantly affects grain yield. *Plant J* 54: 888–898

Pubmed: [Author and Title](#)

Google Scholar: [Author Only](#) [Title Only](#) [Author and Title](#)

Hochholdinger F, Yu P, Marcon C (2018) Genetic Control of Root System Development in Maize. *Trends Plant Sci* 23: 79–88

Pubmed: [Author and Title](#)

Google Scholar: [Author Only](#) [Title Only](#) [Author and Title](#)

Huang G, Liang W, Sturrock CJ, Pandey BK, Giri J, Mairhofer S, Wang D, Muller L, Tan H, York LM, et al (2018) Rice actin binding protein RMD controls crown root angle in response to external phosphate. *Nat Commun* 9: 2346

Pubmed: [Author and Title](#)

Google Scholar: [Author Only](#) [Title Only](#) [Author and Title](#)

Huang P, Jiang H, Zhu C, Barry K, Jenkins J, Sandor L, Schmutz J, Box MS, Kellogg EA, Brutnell TP (2017) Sparse panicle1 is required for inflorescence development in *Setaria viridis* and maize. *Nat Plants* 3: 1–6

Pubmed: [Author and Title](#)

Google Scholar: [Author Only](#) [Title Only](#) [Author and Title](#)

Kiesselbach TA (1949) The structure and reproduction of corn. 50th Anniversary Edition.

Pubmed: [Author and Title](#)

Google Scholar: [Author Only](#) [Title Only](#) [Author and Title](#)

Kremling KAG, Chen SY, Su MH, Lepak NK, Romay MC, Swarts KL, Lu F, Lorant A, Bradbury PJ, Buckler ES (2018) Dysregulation of expression correlates with rare-allele burden and fitness loss in maize. *Nature* 555: 520–523

Pubmed: [Author and Title](#)

Google Scholar: [Author Only](#) [Title Only](#) [Author and Title](#)

Kusmiec A, Schnable PS (2018) FarmCPUpp: Efficient large-scale genomewide association studies. *Plant Direct*. doi: 10.1002/pld3.53

Pubmed: [Author and Title](#)

Google Scholar: [Author Only](#) [Title Only](#) [Author and Title](#)

Lai X, Yan L, Lu Y, Schnable JC (2018) Largely unlinked gene sets targeted by selection for domestication syndrome phenotypes in maize and sorghum. *Plant J*. doi: 10.1111/tpj.13806

Pubmed: [Author and Title](#)

Google Scholar: [Author Only](#) [Title Only](#) [Author and Title](#)

Leiboff S, Li X, Hu HC, Todt N, Yang J, Li X, Yu X, Muehlbauer GJ, Timmermans MCP, Yu J, et al (2015) Genetic control of morphometric diversity in the maize shoot apical meristem. *Nat Commun*. doi: 10.1007/s10071-009-0305-1

Pubmed: [Author and Title](#)

Google Scholar: [Author Only](#) [Title Only](#) [Author and Title](#)

Li H, Peng Z, Yang X, Wang W, Fu J, Wang J, Han Y, Chai Y, Guo T, Yang N, et al (2013) Genome-wide association study dissects the genetic architecture of oil biosynthesis in maize kernels. *Nat Genet* 45: 43–50

Pubmed: [Author and Title](#)

Google Scholar: [Author Only](#) [Title Only](#) [Author and Title](#)

Li L, Hey S, Liu S, Liu Q, McNinch C, Hu HC, Wen TJ, Marcon C, Paschold A, Bruce W, et al (2016) Characterization of maize roothairless6 which encodes a D-type cellulose synthase and controls the switch from bulge formation to tip growth. *Sci Rep* 6: 34395

Pubmed: [Author and Title](#)

Google Scholar: [Author Only](#) [Title Only](#) [Author and Title](#)

Li X, Li X, Fridman E, Tesso TT, Yu J (2015) Dissecting repulsion linkage in the dwarfing gene Dw3 region for sorghum plant height provides insights into heterosis. *Proc Natl Acad Sci* 112: 11823–11828

Pubmed: [Author and Title](#)

Google Scholar: [Author Only](#) [Title Only](#) [Author and Title](#)

Li Z, Mu P, Li C, Zhang H, Li Z, Gao Y, Wang X (2005) QTL mapping of root traits in a doubled haploid population from a cross between upland and lowland japonica rice in three environments. *Theor Appl Genet* 110: 1244–1252

Pubmed: [Author and Title](#)

Google Scholar: [Author Only](#) [Title Only](#) [Author and Title](#)

Liang Q, Cheng X, Mei M, Yan X, Liao H (2010) QTL analysis of root traits as related to phosphorus efficiency in soybean. *Ann Bot* 106: 223–234

Pubmed: [Author and Title](#)

Google Scholar: [Author Only](#) [Title Only](#) [Author and Title](#)

Lin H ying, Liu Q, Li X, Yang J, Liu S, Huang Y, Scanlon MJ, Nettleton D, Schnable PS (2017) Substantial contribution of genetic variation in the expression of transcription factors to phenotypic variation revealed by eRD-GWAS. *Genome Biol*. doi: 10.1186/s13059-017-1328-6

Pubmed: [Author and Title](#)

Google Scholar: [Author Only](#) [Title Only](#) [Author and Title](#)

Lin Z, Li X, Shannon LM, Yeh CT, Wang ML, Bai G, Peng Z, Li J, Trick HN, Clemente TE, et al (2012) Parallel domestication of the Shattering1 genes in cereals. *Nat Genet* 44: 720–724

Pubmed: [Author and Title](#)
Google Scholar: [Author Only Title Only Author and Title](#)

Liu X, Huang M, Fan B, Buckler ES, Zhang Z (2016) Iterative Usage of Fixed and Random Effect Models for Powerful and Efficient Genome-Wide Association Studies. PLoS Genet. doi: 10.1186/1471-2156-13-100

Pubmed: [Author and Title](#)
Google Scholar: [Author Only Title Only Author and Title](#)

Lynch JP (1995) Root Architecture and Plant Productivity. Plant Physiol 109: 7–13

Pubmed: [Author and Title](#)
Google Scholar: [Author Only Title Only Author and Title](#)

Magalhaes J V., Garvin DF, Wang Y, Sorrells ME, Klein PE, Schaffert RE, Li L, Kochian L V. (2004) Comparative mapping of a major aluminum tolerance gene in sorghum and other species in the Poaceae. Genetics 167: 1905–1914

Pubmed: [Author and Title](#)
Google Scholar: [Author Only Title Only Author and Title](#)

Mai CD, Phung NTP, To HTM, Gonin M, Hoang GT, Nguyen KL, Do VN, Courtois B, Gantet P (2014) Genes controlling root development in rice. Rice 7: 30

Pubmed: [Author and Title](#)
Google Scholar: [Author Only Title Only Author and Title](#)

Miao C, Yang J, Schnable JC (2018) Optimising the identification of causal variants across varying genetic architectures in crops. Plant Biotechnol J. doi: 10.1111/pbi.13023

Pubmed: [Author and Title](#)
Google Scholar: [Author Only Title Only Author and Title](#)

Morris GP, Ramu P, Deshpande SP, Hash CT, Shah T, Upadhyaya HD, Riera-Lizarazu O, Brown PJ, Acharya CB, Mitchell SE, et al (2013) Population genomic and genome-wide association studies of agroclimatic traits in sorghum. Proc Natl Acad Sci. doi: 10.1073/pnas.1215985110

Pubmed: [Author and Title](#)
Google Scholar: [Author Only Title Only Author and Title](#)

Nestler J, Liu S, Wen TJ, Paschold A, Marcon C, Tang HM, Li D, Li L, Meeley RB, Sakai H, et al (2014) Roothairless5, which functions in maize (*Zea mays* L.) root hair initiation and elongation encodes a monocot-specific NADPH oxidase. Plant J 79: 729–740

Pubmed: [Author and Title](#)
Google Scholar: [Author Only Title Only Author and Title](#)

Omori F, Mano Y (2007) QTL mapping of root angle in F2 populations from maize 'B73' × teosinte 'Zea luxurians.' Plant Root 1: 57–65

Pace J, Lee N, Naik HS, Ganapathysubramanian B, Lübberstedt T (2014) Analysis of Maize (*Zea mays* L.) Seedling Roots with the High-Throughput Image Analysis Tool ARIA (Automatic Root Image Analysis). PLoS One 9: e108255

Pubmed: [Author and Title](#)
Google Scholar: [Author Only Title Only Author and Title](#)

Park JH, Gail MH, Weinberg CR, Carroll RJ, Chung CC, Wang Z, Chanock SJ, Fraumeni JF, Chatterjee N (2011) Distribution of allele frequencies and effect sizes and their interrelationships for common genetic susceptibility variants. Proc Natl Acad Sci U S A. doi: 10.1073/pnas.1114759108

Pubmed: [Author and Title](#)
Google Scholar: [Author Only Title Only Author and Title](#)

Patel S, Rose A, Meulia T, Dixit R, Cyr RJ, Meier I (2004) Arabidopsis WPP-domain proteins are developmentally associated with the nuclear envelope and promote cell division. Plant Cell 16: 3260–3273

Pubmed: [Author and Title](#)
Google Scholar: [Author Only Title Only Author and Title](#)

Paterson AH, Bowers JE, Bruggmann R, Dubchak I, Grimwood J, Gundlach H, Haberer G, Hellsten U, Mitros T, Poliakov A, et al (2009) The Sorghum bicolor genome and the diversification of grasses. Nature 457: 551–556

Pubmed: [Author and Title](#)
Google Scholar: [Author Only Title Only Author and Title](#)

Peiffer JA, Romay MC, Gore MA, Flint-Garcia SA, Zhang Z, Millard MJ, Gardner CAC, McMullen MD, Holland JB, Bradbury PJ, et al (2014) The genetic architecture of maize height. Genetics 196: 1337–1356

Pubmed: [Author and Title](#)
Google Scholar: [Author Only Title Only Author and Title](#)

Petricka JJ, Schauer MA, Megraw M, Breakfield NW, Thompson JW, Georgiev S, Soderblom EJ, Ohler U, Moseley MA, Grossniklaus U, et al (2012) The protein expression landscape of the Arabidopsis root. Proc Natl Acad Sci 109: 6811–6818

Pubmed: [Author and Title](#)
Google Scholar: [Author Only Title Only Author and Title](#)

Petricka JJ, Winter CM, Benfey PN (2013) Control of Arabidopsis Root Development. Annu Reiew Plant Biol 63: 563–590

Pubmed: [Author and Title](#)
Google Scholar: [Author Only Title Only Author and Title](#)

- Poorter H, Fiorani F, Pieruschka R, Wojciechowski T, van der Putten WH, Kleyer M, Schurr U, Postma J (2016) Pampered inside, pestered outside? Differences and similarities between plants growing in controlled conditions and in the field. *New Phytol* 212: 838–855
Pubmed: [Author and Title](#)
Google Scholar: [Author Only Title Only Author and Title](#)
- Purcell S, Neale B, Todd-Brown K, Thomas L, Ferreira MAR, Bender D, Maller J, Sklar P, de Bakker PIW, Daly MJ, et al (2007) PLINK: A Tool Set for Whole-Genome Association and Population-Based Linkage Analyses. *Am J Hum Genet* 81: 559–575
Pubmed: [Author and Title](#)
Google Scholar: [Author Only Title Only Author and Title](#)
- Quinlan AR, Hall IM (2010) BEDTools: A flexible suite of utilities for comparing genomic features. *Bioinformatics* 26: 841–842
Pubmed: [Author and Title](#)
Google Scholar: [Author Only Title Only Author and Title](#)
- Rauh BL, Basten C, Buckler ES (2002) Quantitative trait loci analysis of growth response to varying nitrogen sources in *Arabidopsis thaliana*. *Theor Appl Genet* 104: 743–750
Pubmed: [Author and Title](#)
Google Scholar: [Author Only Title Only Author and Title](#)
- Richard CAI, Hickey LT, Fletcher S, Jennings R, Chenu K, Christopher JT (2015) High-throughput phenotyping of seminal root traits in wheat. *Plant Methods* 11: 1–11
Pubmed: [Author and Title](#)
Google Scholar: [Author Only Title Only Author and Title](#)
- Schnable JC (2015) Genome Evolution in Maize: From Genomes Back to Genes. *Annu Rev Plant Biol*. doi: 10.1146/annurev-arplant-043014-115604
Pubmed: [Author and Title](#)
Google Scholar: [Author Only Title Only Author and Title](#)
- Schnable JC, Freeling M (2011) Genes identified by visible mutant phenotypes show increased bias toward one of two subgenomes of maize. *PLoS One* 6(3): e17855
Pubmed: [Author and Title](#)
Google Scholar: [Author Only Title Only Author and Title](#)
- Schnable JC, Freeling M, Lyons E (2012) Genome-wide analysis of syntenic gene deletion in the grasses. *Genome Biol Evol* 4: 265–277
Pubmed: [Author and Title](#)
Google Scholar: [Author Only Title Only Author and Title](#)
- Schnable JC, Springer NM, Freeling M (2011) Differentiation of the maize subgenomes by genome dominance and both ancient and ongoing gene loss. *Proc Natl Acad Sci* 108: 4069–4074
Pubmed: [Author and Title](#)
Google Scholar: [Author Only Title Only Author and Title](#)
- Schnable PS, Ware D, Fulton RS, Stein JC, Wei F, Pasternak S, Liang C, Zhang J, Fulton L, Graves TA, et al (2009) The B73 maize genome: Complexity, diversity, and dynamics. *Science* (80-). doi: 10.1126/science.1178534
Pubmed: [Author and Title](#)
Google Scholar: [Author Only Title Only Author and Title](#)
- Schneider CA, Rasband WS, Eliceiri KW (2012) NIH Image to ImageJ: 25 years of image analysis. *Nat Methods* 9: 971–975
Pubmed: [Author and Title](#)
Google Scholar: [Author Only Title Only Author and Title](#)
- Schwarz M (1972) Influence of root crown temperature on plant development. *Plant Soil*. doi: 10.1007/BF02139988
Pubmed: [Author and Title](#)
Google Scholar: [Author Only Title Only Author and Title](#)
- Scutari M (2010) Learning Bayesian Networks with the bnlearn R Package. *J Stat Softw* 35: 1–22
Pubmed: [Author and Title](#)
Google Scholar: [Author Only Title Only Author and Title](#)
- Singh V, van Oosterom EJ, Jordan DR, Messina CD, Cooper M, Hammer GL (2010) Morphological and architectural development of root systems in sorghum and maize. *Plant Soil* 333: 287–299
Pubmed: [Author and Title](#)
Google Scholar: [Author Only Title Only Author and Title](#)
- Suzuki M, Sato Y, Wu S, Kang B-H, McCarty DR (2015) Conserved Functions of the MATE Transporter BIG EMBRYO1 in Regulation of Lateral Organ Size and Initiation Rate. *Plant Cell* 27: 2288–2300
Pubmed: [Author and Title](#)
Google Scholar: [Author Only Title Only Author and Title](#)
- Swigoňová Z, Lai J, Ma J, Ramakrishna W, Llaca V, Bennetzen JL, Messing J (2004) Close split of sorghum and maize genome progenitors. *Genome Res* 14: 1916–1923
Pubmed: [Author and Title](#)
Google Scholar: [Author Only Title Only Author and Title](#)

Thomson MJ, Tai TH, McClung AM, Lai XH, Hinga ME, Lobos KB, Xu Y, Martinez CP, McCouch SR (2003) Mapping quantitative trait loci for yield, yield components and morphological traits in an advanced backcross population between *Oryza rufipogon* and the *Oryza sativa* cultivar Jefferson. *Theor Appl Genet* 107: 479–493

Pubmed: [Author and Title](#)

Google Scholar: [Author Only](#) [Title Only](#) [Author and Title](#)

Topp CN (2016) Hope in Change: The Role of Root Plasticity in Crop Yield Stability. *Plant Physiol* 172: 5–6

Pubmed: [Author and Title](#)

Google Scholar: [Author Only](#) [Title Only](#) [Author and Title](#)

Topp CN, Bray AL, Ellis NA, Liu Z (2016) How can we harness quantitative genetic variation in crop root systems for agricultural improvement? *J Integr Plant Biol* 58: 213–225

Topp CN, Iyer-Pascuzzi AS, Anderson JT, Lee C-R, Zurek PR, Symonova O, Zheng Y, Bucksch A, Mileyko Y, Galkovskiy T, et al (2013) 3D phenotyping and quantitative trait locus mapping identify core regions of the rice genome controlling root architecture. *Proc Natl Acad Sci* 110: E1695–E1704

Pubmed: [Author and Title](#)

Google Scholar: [Author Only](#) [Title Only](#) [Author and Title](#)

Trachsel S, Kaeppler SM, Brown KM, Lynch JP (2013) Maize root growth angles become steeper under low N conditions. *F Crop Res* 140: 18–31

Pubmed: [Author and Title](#)

Google Scholar: [Author Only](#) [Title Only](#) [Author and Title](#)

Trachsel S, Kaeppler SM, Brown KM, Lynch JP (2011) Shovelomics: High throughput phenotyping of maize (*Zea mays* L.) root architecture in the field. *Plant Soil* 341: 75–87

Pubmed: [Author and Title](#)

Google Scholar: [Author Only](#) [Title Only](#) [Author and Title](#)

Uga Y, Sugimoto K, Ogawa S, Rane J, Ishitani M, Hara N, Kitomi Y, Inukai Y, Ono K, Kanno N, et al (2013) Control of root system architecture by DEEPER ROOTING 1 increases rice yield under drought conditions. *Nat Genet* 45: 1097–1102

Pubmed: [Author and Title](#)

Google Scholar: [Author Only](#) [Title Only](#) [Author and Title](#)

Vitha S, Zhao L, Sack FD (2000) Interaction of Root Gravitropism and Phototropism in *Arabidopsis* Wild-Type and Starchless Mutants. *Plant Physiol* 122: 453–462

Pubmed: [Author and Title](#)

Google Scholar: [Author Only](#) [Title Only](#) [Author and Title](#)

Von Behrens I, Komatsu M, Zhang Y, Berendzen KW, Niu X, Sakai H, Taramino G, Hochholdinger F (2011) Rootless with undetectable meristem 1 encodes a monocot-specific AUX/IAA protein that controls embryonic seminal and post-embryonic lateral root initiation in maize. *Plant J*. doi: 10.1111/j.1365-313X.2011.04495.x

Pubmed: [Author and Title](#)

Google Scholar: [Author Only](#) [Title Only](#) [Author and Title](#)

Wang M, Li W, Fang C, Xu F, Liu Y, Wang Z, Yang R, Zhang M, Liu S, Lu S, et al (2018) Parallel selection on a dormancy gene during domestication of crops from multiple families. *Nat Genet*. doi: 10.1038/s41588-018-0229-2

Pubmed: [Author and Title](#)

Google Scholar: [Author Only](#) [Title Only](#) [Author and Title](#)

Wen T-J, Hochholdinger F, Sauer M, Bruce W, Schnable PS (2005) The roothairless1 Gene of Maize Encodes a Homolog of sec3, Which Is Involved in Polar Exocytosis. *PLANT Physiol* 138: 1637–1643

Pubmed: [Author and Title](#)

Google Scholar: [Author Only](#) [Title Only](#) [Author and Title](#)

Wen T-J, Schnable PS (1994) Analysis of mutants of three genes that influence root hair development in *Zea mays* (Gramineae) suggest that root hairs are dispensable. *Am J Bot* 81: 833–842

Pubmed: [Author and Title](#)

Google Scholar: [Author Only](#) [Title Only](#) [Author and Title](#)

Woll K, Borsuk LA, Stransky H, Nettleton D, Schnable PS, Hochholdinger F (2005) Isolation, Characterization, and Pericycle-Specific Transcriptome Analyses of the Novel Maize Lateral and Seminal Root Initiation Mutant rum1. *Plant Physiol* 139: 1255–1267

Pubmed: [Author and Title](#)

Google Scholar: [Author Only](#) [Title Only](#) [Author and Title](#)

Xiao Y, Liu H, Wu L, Warburton M, Yan J (2017) Genome-wide Association Studies in Maize: Praise and Stargaze. *Mol Plant*. doi: 10.1016/j.molp.2016.12.008

Pubmed: [Author and Title](#)

Google Scholar: [Author Only](#) [Title Only](#) [Author and Title](#)

Yamauchi A, KoNo Y, Jiro T (1987) Comparison of root system structures of 13 species of cereals. *Japanese J Crop Sci* 56: 618–631

Pubmed: [Author and Title](#)

Google Scholar: [Author Only](#) [Title Only](#) [Author and Title](#)

Yang N, Lu Y, Yang X, Huang J, Zhou Y, Ai F, Wen W, Liu J, Li J, Yan J (2014) Genome Wide Association Studies Using a New Nonparametric Model Reveal the Genetic Architecture of 17 Agronomic Traits in an Enlarged Maize Association Panel. PLoS Genet. doi: 10.1371/journal.pgen.1004573

Pubmed: [Author and Title](#)

Google Scholar: [Author Only](#) [Title Only](#) [Author and Title](#)

Zhang Y, Marcon C, Tai H, Von Behrens I, Ludwig Y, Hey S, Berendzen KW, Hochholdinger F (2016) Conserved and unique features of the homeologous maize Aux/IAA proteins ROOTLESS with UNDETECTABLE MERISTEM 1 and RUM1-like 1. J Exp Bot 67: 1137–1147

Pubmed: [Author and Title](#)

Google Scholar: [Author Only](#) [Title Only](#) [Author and Title](#)

Zhang Y, Ngu DW, Carvalho D, Liang Z, Qiu Y, Roston RL, Schnable JC (2017) Differentially Regulated Orthologs in Sorghum and the Subgenomes of Maize. Plant Cell. doi: 10.1105/tpc.17.00354

Pubmed: [Author and Title](#)

Google Scholar: [Author Only](#) [Title Only](#) [Author and Title](#)

Zobel RW (2016) Arabidopsis: An adequate model for dicot root systems? Front Plant Sci. doi: 10.3389/fpls.2016.00058

Pubmed: [Author and Title](#)

Google Scholar: [Author Only](#) [Title Only](#) [Author and Title](#)

Zurek PR, Topp CN, Benfey PN (2015) Quantitative Trait Locus Mapping Reveals Regions of the Maize Genome Controlling Root System Architecture. Plant Physiol 167: 1487–1496

Pubmed: [Author and Title](#)

Google Scholar: [Author Only](#) [Title Only](#) [Author and Title](#)